Quantum-mechanical definition of atoms and their mutual interactions in Born-Oppenheimer molecules

J. D. Mills, J. A. Boatz, and P. W. Langhoff

Quantum-Mechanical definition of atoms and their mutual interactions in Born-Oppenheimer molecules

J.D. Mills and J.A. Boatz

Air Force Research Laboratory, 10 East Saturn Blvd., Edwards AFB, CA 93524-7680

P.W. Langhoff*

Department of Chemistry and Biochemistry, University of California,
San Diego, 9500 Gilman Drive, MS 0365, La Jolla, CA, 92093-0365

(Dated: June 1, 2018)

The apparent absence of meaningful assignments of electrons and indistinguishable nuclei to particular atoms in a chemical aggregate would seem to preclude quantum-mechanical definition of atomic Hamiltonian operators *within* molecules and matter. The electronic energies of individual constituent atoms, as well as the interactions between them, are accordingly widely perceived as objectively undefined in molecular quantum theory, requiring additional auxiliary conditions to achieve quantitative specificity, giving rise to a plethora of individual preferences. Here we address the issue of assignments of electrons to atoms within molecules at the Born-Oppenheimer classical "fixed-nuclei" level of theory, and provide thereby quantum-mechanical definitions of atomic operators and of the interactions between them. In the spirit of early work of Longuet-Higgins, a "van-der-Waals" subgroup of the full molecular electronic symmetric group is shown to facilitate assignments of electrons to particular atomic nuclei in a molecule. The orthonormal (Eisenschitz-London) outer-products of atomic eigenstates that provide separable Hilbert space representations of this symmetric subgroup furthermore support totally antisymmetric solutions of the molecular Schrödinger equation. Self-adjoint atomic and atomic-interaction operators within a molecule defined in this way are seen to have *universal* Hermitian matrix representatives and physically significant expectation values in totally antisymmetric molecular eigenstates. Adiabatic Born-Oppenheimer molecular energies emerge naturally from the development in the form of sums of the energies of individual atomic constituents, and of their atomic pairwise interactions, in the absence of additional auxiliary conditions. A detailed and nuanced quantitative description of electronic structure and bonding is provided thereby which includes the interplay between atomic promotion and intereaction energies, common representations of atomic-state hybridization and inter-atomic charge apportionment, potentially measurable multi-atom entanglements upon coherent dissociations of molecules, and other attributes of the development revealed by selected illustrative calculations. These include applications to the ground and electronically excited states of diatomic and triatomic hydrogen molecules, which exhibit significant accommodation among the atomic promotion and interaction energies, as well as entanglements among atomic states, over the entire range of molecular geometries transversed in the course of two- and three-atom dissociations.

Pacs: 03.65.-w, 33.15.-e, 31.10.+z, 33.15.Fm, 61.46.Df, 73.22.-f, 78.67.Bf, 03.65.Aa

I. INTRODUCTION

While it is universally agreed upon that "all things are made of atoms" [1], the notion of an atom in a molecule [2] has been relegated by knowledgeable theorists to the status of a "conceptual construct" or "noumenon", observationally unknowable and without unique definition [3–5]. Quantum-mechanical evaluations of the energies of individual atoms and of their mutual interactions in molecules using molecular eigenfunctions are correspondingly thought to require introduction of subjective auxiliary conditions to achieve specificity in this connection [6], giving rise to unlimited individual preferences, and rendering unique theoretical definition of atomic and bonding energies within molecules continuingly elusive,

even at the Born-Oppenheimer level of theory [7].

Such unresolved fundamental issues are seemingly consequent of the apparent absence of unique quantum-mechanical operator and matrix representatives of the atomic constituents of molecules and matter, the required definitions apparently not in simultaneous accordance with both the principles of quantum theory [8] and Pauli's Exclusion Principle [9]. In this absence, disparate subjective physical interpretations of calculated molecular wave functions, and corresponding quantitative partitions of total electronic energies into atomic and bonding contributions, are a continuing focus of attention, dating from the earliest applications of quantum mechanics to predictions of molecular structure and properties [10–16].

Subjective qualitative opinions offered in this regard are also plentiful [17, 18], ranging from concurrence that atoms in molecules and bonds between them are meaningless illusions [19, 20] to acceptance of the numerous perspectives offered as profitably enriching the subject [21]. Of course, these circumstances have not prevented

*Author to whom correspondence should be addressed: planghoff@mail.ucsd.edu

a plethora of variational and other quantum-mechanical calculations of total energies and other molecular properties employing familiar antisymmetric orbital-product and other less-familiar representations of basis states [22, 23], as well as charge-density-related computational approaches [24, 25], all performed largely in the fixed-nuclei Born-Oppenheimer approximation.

The ever-increasing abundance of molecular calculations provides both impetus and opportunity to pursue physical interpretations of atomic modifications and chemical bonding in molecules in spite of the elusive nature of these quantities. In addition to early considerations of atomic valence-state definitions [10–16], unitary transformations of the molecular orbitals obtained from calculated eigenfunctions have been employed in attempts to identify the presence of physically significant quasi-atomic or bonding character therein, adopting various *ex-post-facto* quantitative criteria for this purpose, such as extreme values of overlap populations or of orbital repulsion energies [26–28]. Additionally, so called natural bonding orbitals have been employed in diagnostic transformations of molecular eigenfunctions, providing plausible charge-density images of atoms and of the bonds between them in molecules [29]. Many other partitions of total and partial charge densities can also be employed in assignments of spatial regions in molecules to constituent atoms or chemical bonds, and to provide estimates of the degree to which individual atoms retain their electronic structural integrity when incorporated in molecules [30–34], including use of information-theory [35] and complexity concepts [36] in charge-density partitions, as well as so-called orbital entanglements in complex electronic systems [37], to mention only some examples to illustrate the absence of a quantum-mechanically unique or generally agreed upon quantitative physical interpretation of molecular electronic charge distributions.

Correspondingly, interest in molecular electronic energy decompositions is already evident in Slater's early Virial-Theorem-based separation of total molecular electronic energies into kinetic and potential energy components [38], and especially in the quantitative comparisons of valence-bond and molecular-orbital methods of Van Vleck, who refers specifically to the interplay between atomic promotion and net bonding energies in the methane molecule [11–14]. Well-known Hellmann-Feynman considerations reveal the forces on individual atomic nuclei in molecules [39, 40], and also provide a basis for their chemical rationalizations [41]. Spatial partitions of molecular one- and two-electron reduced density matrices [6, 42] can also provide total electronic energies expressed as sums of atomic and bonding contributions, whereas energy-decomposition schemes more generally, in conjunction with apportionment of spatial regions to define individual atoms and the bonds between them [26–33], introduce intuitively sensible but ultimately arbitrary fragment components or clusters to obtain quantitative energy expansions [43–59], to cite some representative examples. Recent reviews describe only a small

fraction of the many subjective preferences expressed for interpretations of calculated molecular wave functions, charge distributions, and energy partitions reported to date [60, 61].

Attempts to define meaningful self-adjoint operator representatives of atomic fragments in molecules, as required of dynamical variables by the principles of quantum mechanics [8], soon encounter restrictions consequent of electron indistinguishability [9], which seemingly preclude their unique fixed assignments to particular nuclei in a molecule [2–5]. Specifically, atomic fragment operators do not commute with arbitrary aggregate electron permutations, and so are apparently ill-defined in a molecular context, with Coulomb interaction terms, for example, changing from intra- to inter-atomic character upon electron transpositions. The absence of meaningful partitions of molecular Hamiltonian operators into sums of constituent atomic and interaction-energy operators, and of corresponding representations of atomic and interaction Hamiltonians as Hermitian matrices evaluated with proper molecular wave functions [62], has largely confounded early promising quantum-mechanical atoms-in-molecules formulations [63–65].

The foregoing issues are addressed in the present report by adopting and extending methods introduced largely by Longuet-Higgins [66]. Specifically, a subgroup of the full symmetric group of electron permutations in a molecule is employed to exclude explicit inter-atomic electron permutations [67–69], facilitating assignments of designated electrons to particular nuclei. The representations of this subgroup are constructed in terms of Eisenschitz-London *spectral products* of atomic eigenstates, familiar from early combined studies of covalent and van der Waals forces in molecules [70]. Quantum-mechanical operators for atoms in molecules are obtained in this representation with fixed electron-nuclei assignments made in accordance with those assignments employed in the atomic spectral functions. Totally antisymmetric eigenstates supported in this way provide molecular electronic energies which separate naturally into sums of atomic and pairwise-atomic interaction-energy components upon removal of so-called unphysical non-Pauli eigenstates from the development [71–76].

Molecular (Born-Oppenheimer) Hamiltonian matrices take particularly simple forms in atomic spectral-product representations as sums over universal atomic and pair-interaction Hamiltonian matrices which can be calculated once and for all and retained for repeated applications [71–76]. The corresponding total molecular energies are seen to also take the form of sums over atomic and pairwise-atomic interaction energies, expressed in terms of products of the universal atomic and interaction Hamiltonian matrices and the calculated molecular eigenvectors. Atomic state distributions obtained in this way describe the extent to which individual atoms are excited or de-excited and their electrons apportioned to atomic bonding partners over the molecular volume, whereas the pairwise-atomic terms provide corresponding interaction

energies between constituent atoms.

The theoretical development employing spectral-product representations in definitions of atomic and pairwise-atomic interaction energies is reported in Section II, methods for computational implementation and applications are described in Section III, and illustrative calculations on selected diatomic and triatomic molecules reported in Section IV. Prospects for measurements of interaction energy profiles and corresponding promotion energies employing ultra-fast two- and three-atom dissociation techniques are indicated, and potentially measureable multi-atom entanglements in coherent dissociation of excited electronic states in diatomic and triatomic hydrogen molecules are described.

Concluding remarks in Section V provide additional physical interpretation of the atomic promotion and interaction energies as derived from the spectral product formalism, and on possible measurements of the entangled atoms produced upon coherent dissociations of diatomic and triatomic hydrogen molecules. Finally, Supplemental Material provides an analysis of the early aforementioned atoms-in-molecules methods which identifies the origin of difficulties encountered in their applications [63–65], includes a comprehensive list of these publications as a convenience to the interested reader, and distinguishes these approaches from the spectral theory formalism employed here [71–76].

II. THEORETICAL DEVELOPMENT

Atomic spectral-product representations for molecules are described in Subsection A, and the particular electron-nuclei assignments made in Subsection B are employed in partitioning the molecular Hamiltonian operator into corresponding atomic and atomic-interaction terms. These terms are evaluated as matrix representatives in Subsection C, and total molecular electronic energies obtained from Hamiltonian matrix diagonalization are expressed in terms of atomic and interaction energies in Subsection D. Additional technical aspects of the atomic spectral theory are described elsewhere [71–76].

A. Spectral-product representations

Following Eisenschitz and London [70, 71], the *orthonormal* atomic spectral-product representations employed here are of the "van der Waals" form [77]

$$\boldsymbol{\Phi}(\boldsymbol{r}:\boldsymbol{R}) \equiv$$

$$\left\{ \boldsymbol{\Phi}^{(1)}(\boldsymbol{1}:\boldsymbol{R}_1) \otimes \boldsymbol{\Phi}^{(2)}(\boldsymbol{2}:\boldsymbol{R}_2) \otimes \cdots \boldsymbol{\Phi}^{(N)}(\boldsymbol{n}:\boldsymbol{R}_N) \right\}_{\boldsymbol{o}},$$
$$(1)$$

where the atomic row vectors $\boldsymbol{\Phi}^{(\alpha)}(\boldsymbol{i}:\boldsymbol{R}_\alpha)$ for the atoms α ($= 1, 2, \ldots N$) located at positions $\boldsymbol{R}_\alpha$ formally

contains all their totally antisymmetric electronic eigenstates, with all electrons (n_α) on atoms α designated by the vector $\boldsymbol{i}$ of space and spin coordinates. The vectors $\boldsymbol{r}$ ($= \boldsymbol{1}, \boldsymbol{2}, \ldots \boldsymbol{n}$) and $\boldsymbol{R}$ ($= \boldsymbol{R}_1, \boldsymbol{R}_2, \ldots \boldsymbol{R}_n$) refer collectively to the coordinates of the entire set of molecular electrons (n_t) and to the positions of the atomic nuclei (N), respectively, whereas the subscript $\boldsymbol{o}$ refers to the choice of an "odometer" ordering of the sequence of N-atom product states obtained from the indicated tensor products ($\otimes$) of individual atomic-state row vectors [71–76].

The absence of explicit inter-atomic antisymmetrization insures that the molecular basis of Eq. (1) is orthonormal. Moreover, the basis is complete as written in the limit of closure for descriptions of totally antisymmetric solutions of the Schrödinger equation, in spite of the absence of term-by-term inter-atomic electron antisymmetry in the aggregate spectral products [70]. Furthermore, the basis of Eq. (1) has been shown to contain the totally antisymmetric representation of molecular electrons only once, but to also span other irreducible representations of the symmetric group S_{n_t} [73]. Since the spectral-product basis transforms under the atomic-product subgroup ($S_{n_1} \otimes S_{n_2} \otimes \cdots S_{n_N}$) of S_{n_t} [72], assignments of particular electrons to specific nuclei, made in accordance with the electron assignments of Eq. (1), can be regarded as essentially fixed, as further demonstrated in the sequel.

B. Partitioned molecular Hamiltonian operator

The many-electron Coulomb Hamiltonian operator is written in accordance with the electron assignments of Eq. (1) in the partitioned form [71–76]

$$\hat{H}(\boldsymbol{r}:\boldsymbol{R}) =$$

$$\sum_{\alpha=1}^{N} \hat{H}^{(\alpha)}(\boldsymbol{i}) + \sum_{\alpha=1}^{N-1} \sum_{\beta=\alpha+1}^{N} \hat{V}^{(\alpha,\beta)}(\boldsymbol{i};\boldsymbol{j}:R_{\alpha\beta}), \quad (2)$$

where the atomic Hamiltonian operator for atom α [78]

$$\hat{H}^{(\alpha)}(\boldsymbol{i}) = \sum_{i}^{n_\alpha} \left\{ -\frac{\hbar^2}{2m}\nabla_i^2 - \frac{Z_\alpha e^2}{r_{i\alpha}} + \sum_{i'=i+1}^{n_\alpha} \frac{e^2}{r_{ii'}} \right\} \quad (3)$$

is symmetric in electron coordinates $\boldsymbol{i}$ assigned to atom α, and the interaction term [78]

$$\hat{V}^{(\alpha,\beta)}(\boldsymbol{i};\boldsymbol{j}:R_{\alpha\beta}) =$$

$$\frac{Z_\alpha Z_\beta e^2}{R_{\alpha\beta}} - \sum_{i}^{n_\alpha} \frac{Z_\beta e^2}{r_{i\beta}} - \sum_{j}^{n_\beta} \frac{Z_\alpha e^2}{r_{j\alpha}} + \sum_{i}^{n_\alpha} \sum_{j}^{n_\beta} \frac{e^2}{r_{ij}}$$

$$\equiv \hat{H}^{(\alpha,\beta)}(\boldsymbol{i},\boldsymbol{j}:R_{\alpha\beta}) - \hat{H}^{(\alpha,\beta)}(\boldsymbol{i},\boldsymbol{j}:R_{\alpha\beta} \to \infty) \quad (4)$$

is written and evaluated in the form of the difference of self-adjoint atomic-pair operators [71–74]

$$\hat{H}^{(\alpha,\beta)}(\boldsymbol{i},\boldsymbol{j}:R_{\alpha\beta}) \equiv$$

$$\hat{H}^{(\alpha)}(\boldsymbol{i}) + \hat{H}^{(\beta)}(\boldsymbol{j}) + \hat{V}^{(\alpha,\beta)}(\boldsymbol{i};\boldsymbol{j}:R_{\alpha\beta}), \qquad (5)$$

which are symmetric in electron coordinates $\boldsymbol{i} \oplus \boldsymbol{j}$, with $\boldsymbol{R}_{\alpha\beta} \equiv \boldsymbol{R}_{\beta} - \boldsymbol{R}_{\alpha}$ defining the atomic-position separation vectors. Since all electron coordinates $(\boldsymbol{1},\boldsymbol{2},\ldots\boldsymbol{n})$ are assigned in accordance with the spectral-product representation of Eq. (1), the atomic $\hat{H}^{(\alpha)}(\boldsymbol{i})$ and atomic-pair $\hat{H}^{(\alpha,\beta)}(\boldsymbol{i},\boldsymbol{j}:R_{\alpha\beta})$ fragment Hamiltonian operators of Eqs. (3) to (5) commute with all permutations in the aforementioned atomic-product subgroup of S_{n_t}, proving quantum-mechanical definitions of essentially self-adjoint atomic operators in the support of Eq. (1) [78].

C.   Evaluating the molecular Hamiltonian matrix

The matrix representatives of the molecular Hamiltonian operators of Eqs. (2) to (5) are obtained in the spectral-product basis in the form [71–73]

$$\boldsymbol{H}(\boldsymbol{R}) \equiv \langle \boldsymbol{\Phi}(\boldsymbol{r}:\boldsymbol{R})|\hat{H}(\boldsymbol{r}:\boldsymbol{R})|\boldsymbol{\Phi}(\boldsymbol{r}:\boldsymbol{R})\rangle$$

$$= \sum_{\alpha=1}^{N} \boldsymbol{H}^{(\alpha)} + \sum_{\alpha=1}^{N-1}\sum_{\beta=\alpha+1}^{N} \boldsymbol{V}^{(\alpha,\beta)}(\boldsymbol{R}_{\alpha\beta}), \qquad (6)$$

where the atomic Hamiltonian matrices are

$$\boldsymbol{H}^{(\alpha)} = \left\{ \boldsymbol{I}^{(1)} \otimes \boldsymbol{I}^{(2)} \otimes \cdots \boldsymbol{\epsilon}^{(\alpha)} \otimes \cdots \boldsymbol{I}^{(N)} \right\}_{\boldsymbol{o}} \qquad (7)$$

and the pairwise-atomic interaction Hamiltonian matrices are

$$\boldsymbol{V}^{(\alpha,\beta)}(\boldsymbol{R}_{\alpha\beta}) =$$

$$\left\{ \boldsymbol{I}^{(1)} \otimes \boldsymbol{I}^{(2)} \otimes \cdots \boldsymbol{v}^{(\alpha,\beta)}(\boldsymbol{R}_{\alpha\beta}) \otimes \cdots \boldsymbol{I}^{(N)} \right\}_{\boldsymbol{o}}. \qquad (8)$$

The unit matrices $\boldsymbol{I}^{(\alpha)}$ in Eqs. (7) and (8) arise from the orthonormality of the "bystander" atomic eigenstates in the integrals over the spectral-product representation in Eq. (6), whereas the smaller-dimensioned atomic and atomic-pair matrices in Eqs. (7) and (8),

$$\boldsymbol{\epsilon}^{(\alpha)} \equiv \langle \boldsymbol{\Phi}^{(\alpha)}(\boldsymbol{i}:\boldsymbol{R}_{\alpha})|\hat{H}^{(\alpha)}(\boldsymbol{i})|\boldsymbol{\Phi}^{(\alpha)}(\boldsymbol{i}:\boldsymbol{R}_{\alpha})\rangle \qquad (9)$$

$$\boldsymbol{v}^{(\alpha,\beta)}(\boldsymbol{R}_{\alpha\beta}) \equiv \qquad (10)$$

$$\langle \boldsymbol{\Phi}^{(\alpha,\beta)}(\boldsymbol{i},\boldsymbol{j}:\boldsymbol{R}_{\alpha\beta})|\hat{V}^{(\alpha,\beta)}(\boldsymbol{i},\boldsymbol{j}:R_{\alpha\beta})|\boldsymbol{\Phi}^{(\alpha,\beta)}(\boldsymbol{i},\boldsymbol{j}:\boldsymbol{R}_{\alpha\beta})\rangle,$$

require for their evaluation only the atomic $\boldsymbol{\Phi}^{(\alpha)}(\boldsymbol{i}:\boldsymbol{R}_{\alpha})$ and atomic-pair product functions $\boldsymbol{\Phi}^{(\alpha,\beta)}(\boldsymbol{i},\boldsymbol{j}:\boldsymbol{R}_{\alpha\beta}) \equiv \{\boldsymbol{\Phi}^{(\alpha)}(\boldsymbol{i}:\boldsymbol{R}_{\alpha}) \otimes \boldsymbol{\Phi}^{(\beta)}(\boldsymbol{j}:\boldsymbol{R}_{\beta})\}$, respectively, and the self-adjoint operators of Eqs. (3) to (5) in these smaller atomic and diatomic representations. Faithful matrix representatives [78], which are *universal* computational invariants of the corresponding atomic and interaction-energy operators of Subsection B, are obtained in this way, where the ordering symbol in Eqs. (7) and (8) indicates these larger matrices must be brought into the canonical ordering of Eq. (1) prior to their summation in Eq. (6) [71].

D.   Partitioned molecular energy expression

The molecular energies and Schrödinger eigenstates corresponding to the Hamiltonian matrix of Eq. (6) are obtained from the expression [76]

$$\boldsymbol{E}(\boldsymbol{R}) \equiv \boldsymbol{U_H}^{\dagger}(\boldsymbol{R}) \cdot \boldsymbol{H}(\boldsymbol{R}) \cdot \boldsymbol{U_H}(\boldsymbol{R})$$

$$= \sum_{\alpha=1}^{N} \boldsymbol{E}^{(\alpha)}(\boldsymbol{R}) + \sum_{\alpha=1}^{N-1}\sum_{\beta=\alpha+1}^{N} \boldsymbol{E}^{(\alpha,\beta)}(\boldsymbol{R}), \qquad (11)$$

where the columns of $\boldsymbol{U_H}(\boldsymbol{R})$ contain the eigenvectors which provide the molecular eigenstates in the spectral-product basis; $\boldsymbol{\Psi}(\boldsymbol{r}:\boldsymbol{R}) \equiv \boldsymbol{\Phi}(\boldsymbol{r}:\boldsymbol{R}) \cdot \boldsymbol{U_H}(\boldsymbol{R})$ [72], and the indicated decomposition of the total energy follows employing Eq. (6). That is, in Eq. (11)

$$\boldsymbol{E}^{(\alpha)}(\boldsymbol{R}) \equiv \boldsymbol{U_H}^{\dagger}(\boldsymbol{R}) \cdot \boldsymbol{H}^{(\alpha)} \cdot \boldsymbol{U_H}(\boldsymbol{R}) \qquad (12)$$

is the atomic energy matrix for an atom (α) within a molecule, and

$$\boldsymbol{E}^{(\alpha,\beta)}(\boldsymbol{R}) \equiv \boldsymbol{U_H}^{\dagger}(\boldsymbol{R}) \cdot \boldsymbol{V}^{(\alpha,\beta)}(\boldsymbol{R}_{\alpha\beta}) \cdot \boldsymbol{U_H}(\boldsymbol{R}) \qquad (13)$$

is the pairwise-atomic interaction-energy matrix for atoms (α,β) in a molecule.

In the limit of closure [78],

$$\hat{H}(\boldsymbol{r}:\boldsymbol{R})\boldsymbol{\Phi}(\boldsymbol{r}:\boldsymbol{R}) \rightarrow \boldsymbol{\Phi}(\boldsymbol{r}:\boldsymbol{R}) \cdot \boldsymbol{H}(\boldsymbol{R}), \qquad (14)$$

the molecular Hamiltonian matrix of Eq. (6) can be blocked into separate non-interacting physical and unphysical contributions [73]. In this limit, Eq. (11) provides separate Hamiltonian matrices and individual expressions for the physical and unphysical energies, as well as corresponding Schrödinger eigenstates in the basis of Eq. (1).

Since the molecular energy matrix of Eq. (11) is diagonal by construction, the sums of the diagonal terms of the atomic and atomic-pair interaction-energy matrices of Eqs. (12) and (13) *automatically* provide a decomposition of the total energies of the molecular states. The individual atomic and interaction energies on the diagonals

of these matrices are weighted averages of the universal atomic $\boldsymbol{H}^{(\alpha)}$ and atomic-pair $\boldsymbol{V}^{(\alpha,\beta)}(\boldsymbol{R}_{\alpha\beta})$ Hamiltonian matrices over distributions of atomic-state and atomic-pair-state virtual excitations, respectively, as determined by the eigenvector columns of the matrix $\boldsymbol{U_H}(\boldsymbol{R})$.

Accordingly, the diagonal elements of the atomic- and interaction-energy matrices of Eqs. (12) and (13) provide candidates for quantum-mechanical definitions of atomic and pairwise-atomic interaction energies in a molecule at arbitrary molecular configurations $\boldsymbol{R}$. The off-diagonal terms of the matrices of Eqs. (12) and (13) refer to evaluations of individual atomic and interaction-energy operators between *different* molecular eigenstates. The sums of these off-diagonal terms vanish identically, in accordance with Eq. (11), although the individual off-diagonal atomic and interaction-energy terms generally need not vanish at finite values of interatomic separation [79].

III. COMPUTATIONAL IMPLEMENTATION

Methods are described in Subsection A for the removal of unphysical contributions to the formal development of Section II. Expressions for practical calculations of molecular energies and of atomic and interaction energies of atoms in molecules in finite subspace spectral-product representations are reported in Subsection B, and potentially divergent terms appearing in these expressions are identified and removed analytically in definitions of convegent atomic and pairwise-atomic interaction energies reported in Subsection C.

A. Finite-subspace spectral-product representations

Computational implementation of the foregoing formal development must overcome the presence of unphysical contributions to the spectrum of the Hamiltonian matrix in the spectral-product representation, and insure the exact enforcement of antisymmetry in finite-subspace versions of Eq. (1) [80]. Methods have been developed for such purposes in finite atomic spectral-product representations [72–76, 81–83], including a factored exact pair version of the general development which is particularly well suited for calculations of the fragment molecular energies of focus here [74–76, 83]. This approach provides a Hamiltonian matrix identical in *appearance* to Eq. (6), atomic Hamiltonian matrices in the form of those in Eq. (7), and interaction Hamiltonian matrices that depend only on the separation vectors of the individual atomic pairs, as in Eq. (8).

The origins of the expressions reported here can be understood by noting that the isolation of the totally antisymmetric subspace of any spectral product representation of the form of Eq. (1) can be carried out in a numbers of ways, including, in particular, unitary transformation of Hamiltonian matrices proving factored sub-

space spectral-product representations, or, equivalently, by the use of explicitly antisymmetrized representations transformed to spectral-product forms [73].

The isolation of the totally antisymmetric subspace of Eq. (1) in the factored exact pair development is performed in a two-step fashion in which the individual diatomic representations employed in Eq. (10) are first transformed to antisymmetric forms, followed by isolation of the totally antisymmetric subspace of the aggregate basis of Eq. (1) [74–76, 83]. When the antisymmetrized form of the chosen finite subspace of Eq. (1) is made linearly independent, the second or aggregate step of the symmetric group symmetry isolation process takes the form of an overall unitary transformation of the aggregate Hamiltonian matrix constructed in the first step [83]. Consequently, calculations of total aggregate electronic energies in such cases are obtained from aggregate Hamiltonian matrices in forms similar to those of Eqs. (11) to (13), but employing different expressions for the required Hamiltonian matrices of Eqs. (8) and (10).

Following the factored exact pair development [74–76, 83], the Hamiltonian matrix in the chosen finite subspace $\tilde{\boldsymbol{\Phi}}(\boldsymbol{r} : \boldsymbol{R})$ of Eq. (1) takes the form [cf., Eqs. (6) to (10)]

$$\tilde{\boldsymbol{H}}(\boldsymbol{R}) \equiv \langle \tilde{\boldsymbol{\Phi}}(\boldsymbol{r} : \boldsymbol{R})|\hat{H}(\boldsymbol{r} : \boldsymbol{R})|\tilde{\boldsymbol{\Phi}}(\boldsymbol{r} : \boldsymbol{R})\rangle$$

$$= \sum_{\alpha=1}^{N} \tilde{\boldsymbol{H}}^{(\alpha)} + \sum_{\alpha=1}^{N-1} \sum_{\beta=\alpha+1}^{N} \tilde{\boldsymbol{V}}^{(\alpha,\beta)}(\boldsymbol{R}_{\alpha\beta}), \qquad (15)$$

where the atomic and interaction Hamiltonian matrices are finite-dimensioned versions of Eqs. (7) and (8). Although Eqs. (7) and (9) are otherwise unchanged, $\boldsymbol{v}^{(\alpha,\beta)}(\boldsymbol{R}_{\alpha\beta})$ in Eq. (8) is given in the factored exact pair form by the finite-subspace expression [cf., Eq.(4)]

$$\tilde{\boldsymbol{v}}^{(\alpha,\beta)}(\boldsymbol{R}_{\alpha\beta}) \equiv$$

$$\tilde{\boldsymbol{u}}_{\boldsymbol{s}}^{(\alpha,\beta)}(\boldsymbol{R}_{\alpha\beta}) \cdot \tilde{\boldsymbol{h}}_{\boldsymbol{s}}^{(\alpha,\beta)}(\boldsymbol{R}_{\alpha\beta}) \cdot \tilde{\boldsymbol{u}}_{\boldsymbol{s}}^{(\alpha,\beta)}(\boldsymbol{R}_{\alpha\beta})^{\dagger} - (\boldsymbol{\epsilon}^{(\alpha)} + \boldsymbol{\epsilon}^{(\beta)})$$
$$(16)$$

in place of Eq. (10), where

$$\tilde{\boldsymbol{h}}_{\boldsymbol{s}}^{(\alpha,\beta)}(\boldsymbol{R}_{\alpha\beta}) \equiv$$

$$\langle \tilde{\boldsymbol{\Phi}}_{\boldsymbol{s}}^{(\alpha,\beta)}(\boldsymbol{i},\boldsymbol{j} : \boldsymbol{R}_{\alpha\beta})|\hat{H}^{(\alpha,\beta)}(\boldsymbol{i},\boldsymbol{j} : R_{\alpha\beta})|\tilde{\boldsymbol{\Phi}}_{\boldsymbol{s}}^{(\alpha,\beta)}(\boldsymbol{i},\boldsymbol{j} : \boldsymbol{R}_{\alpha\beta})\rangle$$
$$(17)$$

is the (α,β) atomic-pair Hamiltonian matrix, evaluated employing an explicitly antisymmetrized orthonormal finite-subspace diatomic representation $\tilde{\boldsymbol{\Phi}}_{\boldsymbol{s}}^{(\alpha,\beta)}(\boldsymbol{i},\boldsymbol{j} : \boldsymbol{R}_{\alpha\beta})$ [74–76, 83]. The second term in Eq. (16) is as in Eq. (4), whereas the unitary matrix $\tilde{\boldsymbol{u}}_{\boldsymbol{s}}^{(\alpha,\beta)}(\boldsymbol{R}_{\alpha\beta})$ there is obtained from the metric matrix $\tilde{\boldsymbol{s}}^{(\alpha,\beta)}(\boldsymbol{R}_{\alpha\beta})$ of the non-orthogonal antisymmetrized pair representation [84]. This transformation is employed to both construct the explicitly antisymmetrized orthonormal finite-subspace

diatomic representation and to recover the corresponding orthonormal finite-subspace spectral-product representation $\tilde{\boldsymbol{\Phi}}(\boldsymbol{r} : \boldsymbol{R})$ of the interaction energy matrix of Eq. (8) in closure [83].

In the more general variants of the two-step antisymmetrization development [74–76, 83], the form of Eq. (15) is retained but the atomic- and interaction-energy matrices there become functions of the position coordinates ($\boldsymbol{R}$) of all the atoms in the molecule, consequent of the dressing of atomic pair matrices by the aggregate antisymmetry enforcement. Since the condition for validity of Eqs. (15) to (17) for calculations of aggregate energies requires only the familiar linear independence of the totally antisymmetrized form of the finite spectral-product representation employed [74–76, 83], the calculated *energies* reported here are identical with those obtained from the aforementioned more general computational approaches, but avoid the additional complications entailed therein [76].

B. Partitioned molecular energies in finite subspaces

Energy expressions corresponding to those of Eqs. (11) to (13) are obtained employing the finite-subspace matrices of Eqs. (16) and (17) and the unitary matrix $\tilde{\boldsymbol{U}}_{\boldsymbol{H}}(\boldsymbol{R})$ that diagonalizes the corresponding total Hamiltonian matrix of Eq. (15). The total electronic energy $\tilde{E}_i(\boldsymbol{R})$ of a particular *molecular* eigenstate (i) obtained in this way takes the form of a sum of atomic energies for the constituent atoms and an atomic-pairwise sum of interaction energies [cf., Eq.(11)]

$$\tilde{E}_i(\boldsymbol{R}) = \sum_{\alpha=1}^{N} \tilde{E}_i^{(\alpha)}(\boldsymbol{R}) + \sum_{\alpha=1}^{N-1} \sum_{\beta=\alpha+1}^{N} \tilde{E}_i^{(\alpha,\beta)}(\boldsymbol{R}). \quad (18)$$

The individual energy term $\tilde{E}_i^{(\alpha)}(\boldsymbol{R})$ for atom α in a particular molecular eigenstate i is provided by the diagonal entry of the finite-subspace versions $\tilde{\boldsymbol{E}}^{(\alpha)}(\boldsymbol{R})$ of the atomic energy matrices of Eq. (12) in the form

$$\tilde{E}_i^{(\alpha)}(\boldsymbol{R}) \equiv \{\tilde{\boldsymbol{E}}^{(\alpha)}(\boldsymbol{R})\}_{ii} = \sum_{k=1}^{N_{sp}} \{\tilde{\boldsymbol{H}}^{(\alpha)}\}_{kk} |\{\tilde{\boldsymbol{U}}_{\boldsymbol{H}}(\boldsymbol{R})\}_{ki}|^2$$

$$= \sum_{k=1}^{N^{(\alpha)}} \tilde{\epsilon}_k^{(\alpha)} |\{\tilde{\boldsymbol{u}}_{\boldsymbol{H}}^{(\alpha)}(\boldsymbol{R})\}_{ki}|^2, \quad (19)$$

where N_{sp} is the dimension of the aggregate finite spectral-product representation, $N^{(\alpha)}$ is the dimension of the atomic representation $\tilde{\boldsymbol{\Phi}}^{(\alpha)}(i : \boldsymbol{R}_\alpha)$, and $\tilde{\boldsymbol{u}}_{\boldsymbol{H}}^{(\alpha)}(\boldsymbol{R})$ is the reduced "one-atom" density matrix derived from the unitary spectral-product solution matrix $\tilde{\boldsymbol{U}}_{\boldsymbol{H}}(\boldsymbol{R})$ [71] for atom α, employing Eq. (7) in the last line.

Similarly, the diagonal term $\tilde{E}_i^{(\alpha,\beta)}(\boldsymbol{R})$ of the finite-subspace version $\tilde{\boldsymbol{E}}^{(\alpha,\beta)}(\boldsymbol{R})$ of the interaction-energy matrix of Eq. (13) for atoms α and β takes the form

$$\tilde{E}_i^{(\alpha,\beta)}(\boldsymbol{R}) \equiv \{\tilde{\boldsymbol{E}}^{(\alpha,\beta)}(\boldsymbol{R})\}_{ii} =$$

$$\sum_{k=1}^{N_{sp}} \sum_{l=1}^{N_{sp}} \{\tilde{\boldsymbol{U}}_{\boldsymbol{H}}(\boldsymbol{R})^\dagger\}_{ik} \{\tilde{\boldsymbol{V}}^{(\alpha,\beta)}(\boldsymbol{R}_{\alpha\beta})\}_{kl} \cdot \{\tilde{\boldsymbol{U}}_{\boldsymbol{H}}(\boldsymbol{R})\}_{li} =$$

$$\sum_{k=1}^{N^{(\alpha)}} \sum_{l=1}^{N^{(\beta)}} \{\tilde{\boldsymbol{u}}_{\boldsymbol{H}}^{(\alpha,\beta)}(\boldsymbol{R})^\dagger\}_{ik} \{\tilde{\boldsymbol{v}}^{(\alpha,\beta)}(\boldsymbol{R}_{\alpha\beta})\}_{kl} \cdot \{\tilde{\boldsymbol{u}}_{\boldsymbol{H}}^{(\alpha,\beta)}(\boldsymbol{R})\}_{li}, \quad (20)$$

where $\tilde{\boldsymbol{u}}_{\boldsymbol{H}}^{(\alpha,\beta)}(\boldsymbol{R})$ is the reduced "two-atom" density matrix for the atoms α and β derived from the matrix $\tilde{\boldsymbol{U}}_{\boldsymbol{H}}(\boldsymbol{R})$ [71], and the sums in the last line are over the individual product states describing the atomic-pairwise interaction Hamiltonian matrix of Eqs. (16) and (17).

Further reduction of the expression of Eq. (20) can be made by diagonalizing the atomic-pairwise Hamiltonian matrix $\tilde{\boldsymbol{h}}_{\boldsymbol{s}}^{(\alpha,\beta)}(\boldsymbol{R}_{\alpha\beta})$ appearing in Eqs. (16) and (17), and redefining the two-atom density matrix to include this additional unitary matrix. In this way, an energy expression is obtained involving a weighted sum of scalar atomic-pairwise interaction-energy curves in a form similar to the weighted sum of atomic energies of Eq. (19).

C. Quantum-mechanical definition of atomic promotion and atomic pairwise interaction energies in molecules

Although the preceeding analysis is satisfactory in its essential features, the atomic energy terms of Eq. (19) and the interaction-energy terms of Eq. (20) do not individually converge to finite values, in spite of the fact that the total molecular energies of Eq. (18) converge to variationally correct values in a suitable closure limit [78]. It is easily established, both computationally and analytically, that these divergences arise from continuum atomic contributions to Eqs. (19) and (20), such terms cancelling exactly in the total energy sum of Eq. (18) [86]. Moreover, it is clear on physical grounds that only bound atomic states are sensibly included in the definition of atomic promotion in any event, with continuum contributions referring to ionized molecular states [10–16].

When these diverging terms are eliminated analytically from the expression of Eq. (18), the finite promotion energies for individual atoms are still given by the expression of Eq. (19) but the atomic Hamiltonian matrix therein is replaced by its discrete-state portion only $\tilde{\boldsymbol{H}}^{(\alpha)} \rightarrow \tilde{\boldsymbol{H}}_{\boldsymbol{d}}^{(\alpha)}$ [86]. Similarly, the atomic-pairwise Hamiltonian matrix retains the form of Eq. (20) but is now finite when the diverging terms in the matrix
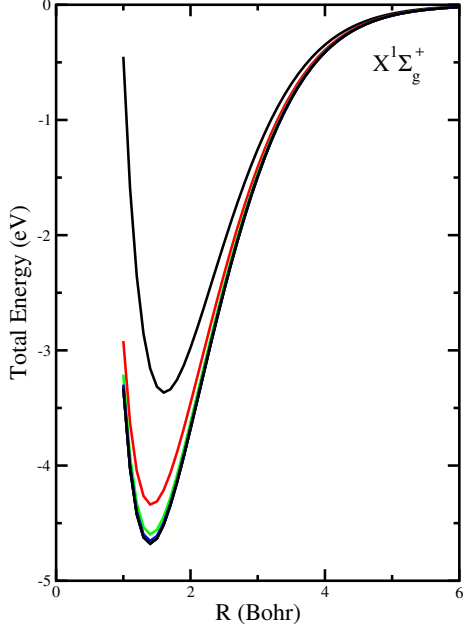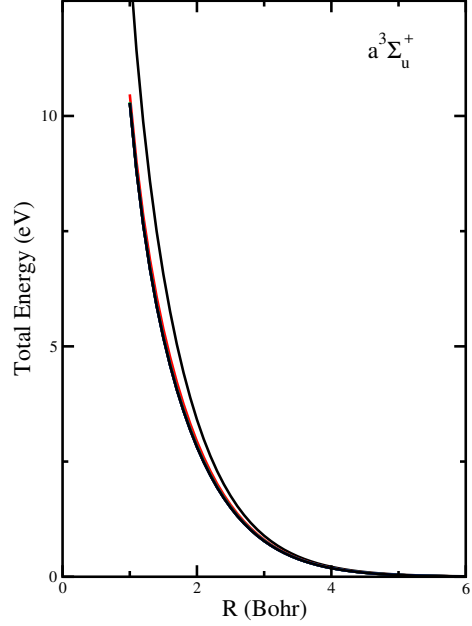
FIG. 1: Convergence of the total electronic energy of the $X^1\Sigma_g^+$ ground state in molecular hydrogen (H$_2$), calculated employing increasing numbers (196 to 7,396) of products of k = 1 to 9 sets of (s,p,d)$_k$ exact hydrogenic and eigenorbitals constructed in even-tempered Slater basis sets [87, 88].

FIG. 2: Convergence of the total electronic energy of the $a^3\Sigma_u^+$ first excited state in molecular hydrogen (H$_2$), calculated employing increasing numbers (196 to 7,396) of products of k = 1 to 9 sets of (s,p,d)$_k$ exact hydrogenic and eigenorbitals constructed in even-tempered Slater basis sets [87, 88].

$\tilde{V}^{(\alpha,\beta)}(\boldsymbol{R}_{\alpha\beta})$ are cancelled analytically by corresponding atomic terms; $\tilde{V}^{(\alpha,\beta)}(\boldsymbol{R}_{\alpha\beta}) \rightarrow \tilde{V}_{int}^{(\alpha,\beta)}(\boldsymbol{R}_{\alpha\beta})$ and $\tilde{\boldsymbol{v}}^{(\alpha,\beta)}(\boldsymbol{R}_{\alpha\beta}) \rightarrow \tilde{\boldsymbol{v}}_{int}^{(\alpha,\beta)}(\boldsymbol{R}_{\alpha\beta})$ [86].

Accordingly, the total molecular Hamiltonian matrix retains the form of Eq. (18) but the promotion energy of an atom α in a molecular state i is [cf., Eq (19)]

$$\tilde{E}_i^{(\alpha)}(\boldsymbol{R}) = \sum_{k=1}^{N_d^{(\alpha)}} \tilde{\epsilon}_k^{(\alpha)} \, |\{\tilde{\boldsymbol{u}}_H^{(\alpha)}(\boldsymbol{R})\}_{ki}|^2, \qquad (21)$$

with $N_d^{(\alpha)}$ the number of bound atomic states for the atom α, and the interaction energy is [cf., Eq. (20)]

$$\tilde{E}_i^{(\alpha,\beta)}(\boldsymbol{R}) \equiv \qquad (22)$$

$$\sum_{k=1}^{N^{(\alpha)}} \sum_{l=1}^{N^{(\beta)}} \{\tilde{\boldsymbol{u}}_H^{(\alpha,\beta)}(\boldsymbol{R})^\dagger\}_{ik} \cdot \{\tilde{\boldsymbol{v}}_{int}^{(\alpha,\beta)}(\boldsymbol{R}_{\alpha\beta})\}_{kl} \cdot \{\tilde{\boldsymbol{u}}_H^{(\alpha,\beta)}(\boldsymbol{R})\}_{li}$$

where $\tilde{\boldsymbol{v}}_{int}^{(\alpha,\beta)}(\boldsymbol{R}_{\alpha\beta})$ excludes divergent terms [86].

It should be noted that extraction of the singular terms in Eqs. (19) and (20) leave the total electronic energies given by Eq. (18) invariant to this procedure.

IV. ILLUSTRATIVE APPLICATIONS

Calculations with the present formalism are reported of total electronic energies and of the atomic-promotion and pairwise interaction energies in diatomic and triatomic hydrogen molecules. Accurate representations of selected electronic states are obtained in providing quantitative illustrations of the theoretical development in these prototypically important cases.

A. Total electronic, atomic promotion, and interaction energies in diatomic hydrogen molecules

Calculations are reported in the classic cases of the homopolar bond in the ground singlet $X^1\Sigma_g^+$ electronic state and of the antibond in the triplet $a^3\Sigma_u^+$ state of moleculer hydrogen H$_2$. Monotonic convergence is obtained to values of the total electronic energies (Figures 1 and 2), atomic-promotion energies (Figures 3 and 4), and chemical-interaction energies (Figures 5 and 6) in these familiar attractive and repulsive states employing large numbers of atomic-product molecular basis functions. These are chosen in the form of atomic hydrogen eigenorbitals constructed in unrestricted products of k = 1 to 9 sets of (s,p,d)$_k$ atomic basis orbitals on the
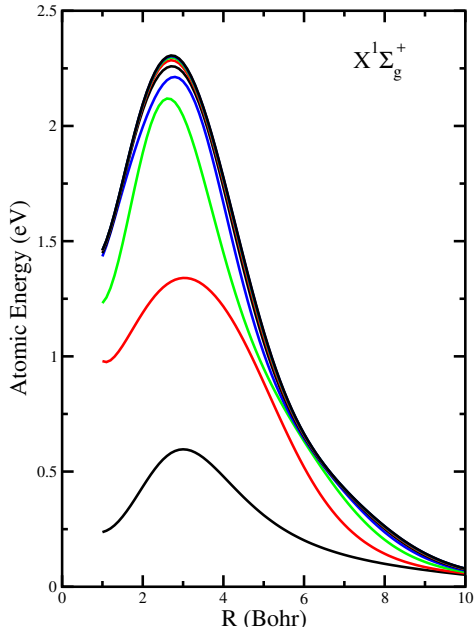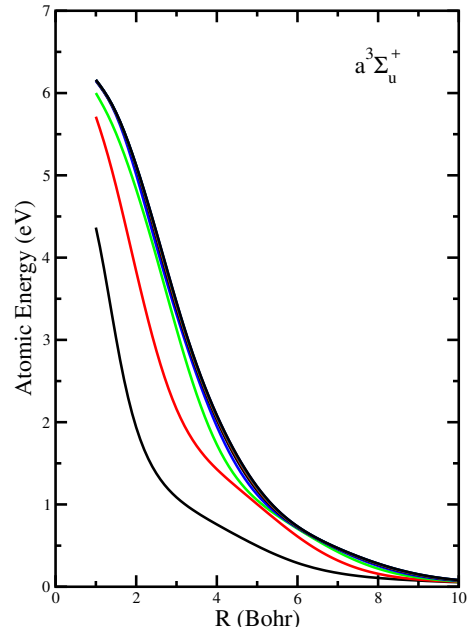
FIG. 3: Convergence of the atomic promotion energy of hydrogen atoms within the $X^1\Sigma_g^+$ state in molecular hydrogen, calculated employing increasing numbers (196 to 7,396) of products of k=1 to 9 sets of $(s,p,d)_k$ exact hydrogenic and eigenorbitals constructed in even-tempered Slater basis sets [87, 88].

FIG. 4: Convergence of atomic promotion energy of hydrogen atoms within the $a^3\Sigma_u^+$ state in molecular hydrogen, calculated employing increasing numbers (196 to 7,396) of products of k=1 to 9 sets of $(s,p,d)_k$ exact hydrogenic and eigenorbitals constructed in even-tempered Slater basis sets [87, 88].

two nuclear centers. The first set (k=1) of orbitals are the lowest-lying fourteen exact hydrogen atom orbitals (1s,2s,2p,3s,3p,3d), providing 196 orbital-product states, whereas the additional $(s,p,d)_k$ basis orbital sets each contain nine (1s(1),3p(3),3d(5)) even-tempered Slater orbitals having exponents $\alpha_k = \alpha_0 \beta^{(k-2)}$, for k = 2 to 9, where $\beta = 1.7$ and $\alpha = 0.001$ [87, 88]. This combined set of Slater orbitals spans 86 individual hydrogen eigenorbitals on each center, providing up to 7,396 atomic-product molecular hydrogen basis states.

In Figures 1 and 2 are shown calculated total electronic energy curves, including the $1/R$ nuclear repulsion term, of the $X^1\Sigma_g^+$ and $a^3\Sigma_u^+$ states in H$_2$ as functions of nuclear separation. These curves converge monotonically from above with increasing basis set (k = 1 to 9) to values in exact agreement with results obtained from conventional valence-bond variational calculations in the same basis sets [89]. In the present development the electronic energy curves of Eq. (18) in Figures 1 and 2 are further partitioned in the calculations into atomic promotion energies for the two atoms [Eq. (21)] and chemical interaction energies between the atoms [Eq.(22)] in the absence of additional auxiliary conditions.

In Figures 3 and 4 are shown atomic promotion energy curves of hydrogen atoms within diatomic hydrogen in

the $X^1\Sigma_g^+$ and $a^3\Sigma_u^+$ states as functions of nuclear separation, obtained from Eq. (21). These curves are seen to converge from *below* with increasing basis set to limiting values which provide quantitative representations of the contributions of the two atoms to the total molecular electronic energy. It is easily understood from Eq. (21) that the lower limit of the promotion energy of an atom in a molecule from its ground electronic state is zero, whereas an upper limit is provided by the first ionization potential of the atom.

Evidently, the hydrogen atom promotion energy in the ground electronic state of Figure 3 is a small fraction ($\leq$ 17%) of the maximum allowed value (13.6 eV), and decreases at both larger and smaller R values, whereas in the repulsive state of Figure 4 the promotion energy rises to a larger fraction ($\leq$ 45%) of the maximum allowed, and also lowers at larger and smaller separations (not shown). The R $\rightarrow$ 0 behaviors are related to the electronic energies of the two molecular states in the united-atom (He) limits, with the ground $(1s^2)^1S$ atomic He state limit of the $X^1\Sigma_g^+$ molecular curve at -79.0 eV lying significantly below the excited $(1s2p)^3P$ state -55.5 eV united atom limit of the $a^3\Sigma_u^+$ curve, both states lying well below the energy of two ground-state hydrogen atoms (-27.2 eV) [90]. The atomic basis sets employed here do not provide optimal representations of the atomic orbitals in
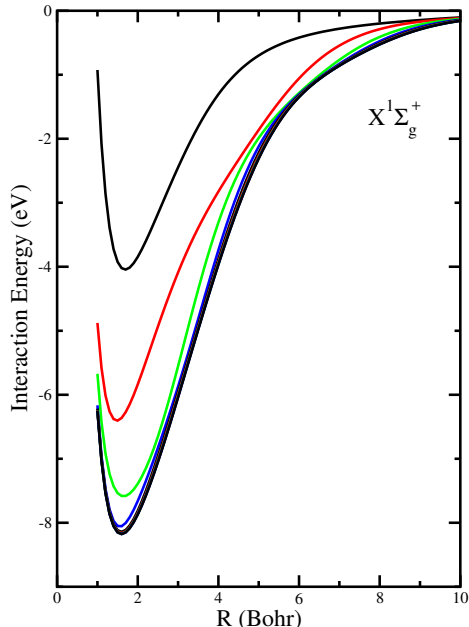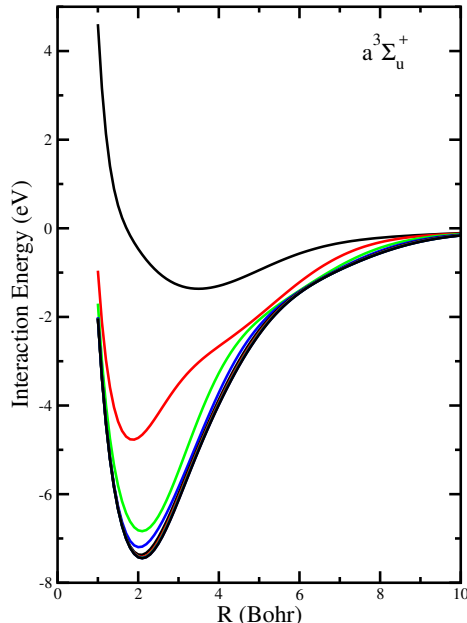
FIG. 5: Convergence of mutual interaction energy between hydrogen atoms in the $X^1\Sigma_g^+$ state of molecular hydrogen, calculated employing increasing numbers (196 to 7,396) of products of k=1 to 9 sets of $(s,p,d)_k$ exact hydrogenic and eigenorbitals constructed in even-tempered Slater basis sets [87, 88].

FIG. 6: Convergence of mutual interaction energy between hydrogen atoms in the $a^3\Sigma_u^+$ state of molecular hydrogen, calculated employing increasing numbers (196 to 7,396) of products of k=1 to 9 sets of $(s,p,d)_k$ exact hydrogenic and eigenorbitals constructed in even-tempered Slater basis sets [87, 88].

He. Nevertheless, the total electronic energies of Figures 1 and 2 and the atomic energies of Figures 3 and 4 obtained in the $R \to 0$ limit show energy lowerings in accord with these well known atomic values [90].

In Figures 5 and 6 are shown interaction energies between the two atoms in the $X^1\Sigma_g^+$ ground state and the first excited $a^3\Sigma_u^+$ state of molecular hydrogen as functions of atomic separation, calculated employing Eq. (22) and the atomic-product molecular basis states described above. These curves evidently exhibit monotonic convergence from above to results that differ quantitatively and qualitatively from the corresponding total electronic energy curves of Figures 1 and 2.

The converged minimum interaction energy in the ground molecular state of Figure 5 is seen to be significantly lower than the adiabatic bond energy of the potential curve of Figure 1 (-8.2 eV vs. -4.7 eV), compensating for the positive atomic promotion energy of Figure 3 for this state in providing the correct total energy curve in accordance with Eq. (18). Additionally, the interaction energy curve is significantly broader than the total energy curve, in accordance with the atomic promotion energy curve extending over a similarly broad spatial extent.

In contrast to the adiabatic total energy curve of Figure 2, the interaction-energy curve of Figure 6 for the "re-

pulsive" triplet state shows a suprisingly deep and broad well. This behavior compensates for the large promotion energies of the two atoms shown in Figure 4 in providing the total electronic energy of Figure 2. This interaction energy curve also extends over a significant range of R values, in accord with the corresponding range of the atomic promotion energies in Figure 4. These accommodating behaviors for both singlet and triplet states verify the numerical accuracy of the calculations, insuring that the separate contributions from promotion and interaction energies sum correctly to the total energy curves.

The interaction energy curves of Figure 5 and 6 provide new information complementary to that of the total energy curves of Figures 1 and 2, which refer to the familiar adiabatic work required to dissociate H_2 from a separation R into two ground-state (1s) hydrogen atoms. By contrast, in spite of being calculated under adiabatic quantum-mechanical conditions, the curves of Figure 5 and 6 provide approximations to the work required or released upon the "sudden" dissociation of H_2 into the promoted atomic states associated with Figures 3 and 4, in the absence of atomic electronic relaxation. The curves of Figures 5 and 6 include in the dissociation process the additional work associated with atomic promotion over and above that depicted in Figures 1 and 2.
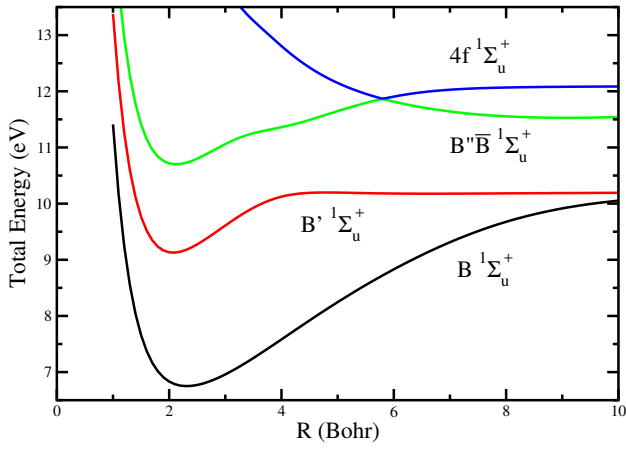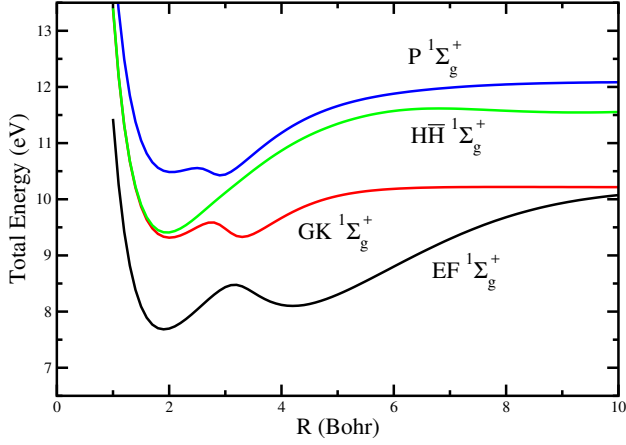
FIG. 7: **Upper Panel**: Total electronic energy curves for the $EF^1\Sigma_g^+$, $GK^1\Sigma_g^+$, $H\bar{H}^1\Sigma_g^+$, and $P^1\Sigma_g^+$ electronic states in diatomic molecular hydrogen (H_2). **Lower Panel**: Total energy curves for the $B^1\Sigma_u^+$, $B'^1\Sigma_u^+$, $B''\bar{B}^1\Sigma_u^+$, and $4f^1\Sigma_u^+$ electronic states of diatomic molecular hydrogen (H_2), all calculated as described in the text.

FIG. 8: **Upper Panel**: Atomic promotion energy curves for excited diatomic hydrogen molecule states of gerade summetry. **Lower Panel**: Atomic-pair interaction energy curves for excited diatomic hydrogen molecule states of gerade summetry, all calculated as described in the text

That is, while the adiabatic curves refer to a range of atomic valence states traversed in the course of adiabatic dissociation, the curves of Figures 5 and 6 refer to specific atomic valence states frozen in the course of sudden dissociations. In principle, suitably designed very-short-timescale photodissociation measurements could be performed to reveal such sudden dissociation energies.

B. Atomic entanglements in the excited states of molecular hydrogen

In the limit of large R, the dissociation products of the two molecular hydrogen states considered above ultimately approach pairs of 1s atomic hydrogen atoms in singlet and triplet spin coupling, as seen in Figures 1 and 2. In contrast, excited states of diatomic molecules can dissociate to mixed ground and excited atomic states or pairs of possibly degenerate atomic states. These can exhibit aspects of entanglements upon coherent dissociation [92–97], issues discussed previously in various connections, including dissociations of diatomic hydrogen molecules [98–103].

Detailed calculations of atomic entanglement phenomena are reported here in the cases of electroncally excited states of diatomic hydrogen molecules having singlet gerade and ungerade symmetries, including in particular the $EF^1\Sigma_g^+$, $GK^1\Sigma_g^+$, $H\bar{H}^1\Sigma_g^+$, and $P^1\Sigma_g^+$ gerade states, and the $B^1\Sigma_u^+$, $B'^1\Sigma_u^+$, $B''\bar{B}^1\Sigma_u^+$, and $4f^1\Sigma_u^+$ ungerade states [104–108]. The $EF^1\Sigma_g^+$, $H\bar{H}^1\Sigma_g^+$, $B'^1\Sigma_u^+$, and $B''\bar{B}^1\Sigma_u^+$ states are commonly termed "ionic" consequent of the corresponding wide potential wells and the contribution of $H^+ + H^-$ charge-transfer configurations in model quantum chemical calculations. By contrast, representations of the form of Eq. (1) include only products of neutral atomic states in providing support for accurate quantum mechanical calculations, which, however,

also describe charge transfer phenomena [71–77, 83]. Explict charge-transfer configurations, when *employed with* atomic product representations which already include such terms [70, 71], lead to linear dependence, confirming therebye the well-known physical equivalence of the two apparently disparate forms of representation [70–75, 83].

In Figure 7 are shown the total energy curves of these gerade and ungerade excited diatomic hydrogen states, calculated employing the atomic hydrogen orbital representations described in the ground-state calculations reported in Figure 1 to 6 above. The atomic spectral-product representations employed in the calculations of Figure 7 comprise totals of 4,624 eigenorbital products in each symmetry, ensuring convergence of the curves shown to values in good agreement with previously reported highly accurate results [106–108].

In Figures 8 and 9 are shown the atomic promotion and atomic-pair interaction energies corresponding to the two sets of total energy curves of Figure 7. The former figures are aligned to emphasize the interplay between promotion and interaction energy terms in Eq. (18). Specifically, it is seen from Figures 8 and 9 that variations in the atomic promotion energies of the gerade and ungerade states considered are accompanied by corresponding variations in the interaction energies in determining the forms of the total electroniuc energy curves of Figure 7.

Of particular interest in Figure 8 are the rather large variations in the atomic promotion energies, which are comparable to those of the interaction energies, particularly in the EF and GK states, indicating that the double-well structures of the corresponding total energy curves are consequences of both atomic promotions and bonding intreractions. Similar remarks also apply to the atomic promotion and interaction energy curves of Figure 9, particularly for the lowest lying ungerade state, having a deep well.

The effects of the avoided curve crossing between the two highest lying ungerade electronic energy curves of Figure 7 are quite apparent in the corresponding atomic promotion and interaction energy curves of Figure 9. Although the total energy curves appear to actually cross in Figure 7, detailed examination of the $R \approx 6.0$ Bohr region of the Lower Panel of Figure 7 shows an avoidance of approximately 0.04 eV between the two curves. The curves of Figure 9 clearly indicate the effects of the avoidance present at ≈ 6 Bohr in the total energy curves, confirming the diagonostic power of the energy partitioning of Eq. (18) in this case.

The features evident in the calculated total, atomic promotion, and interaction energy curves of Figures 7, 8, and 9 for the excited H_2 states considered are in contrast to those of Figure 1 to 6 for the lowest lying singlet and triplet states in H_2, which depict largely smooth unstructured variations with bond separation.
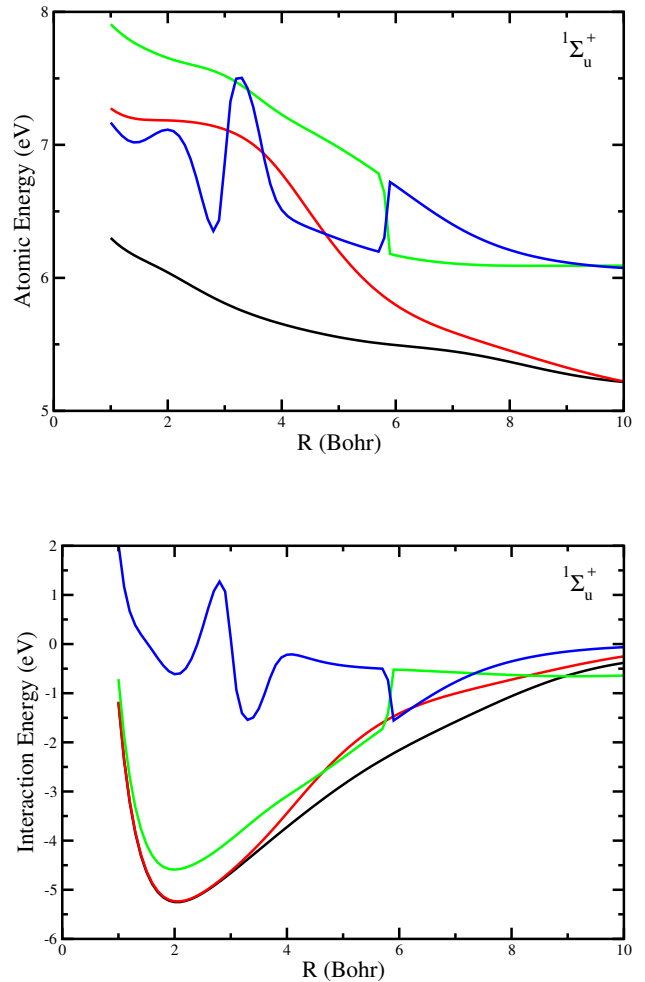

FIG. 9: **Upper Panel**: Atomic promotion energy curves for excited diatomic hydrogen molecule states of ungerade summetry. **Lower Panel**: Atomic-pair interaction energy curves for excited diatomic hydrogen molecule states of ungerade summetry, all calculated as described in the text.

C.   Atomic state promotion probabilities in diatomic hydrogen molecules

Reduced "one-atom" and "two-atom" density matrices [71], employed in Section III B, Eqs. (19) and (20), provide quantitive measures of the contributions of the various basis states of a given atom to its atomic and atomic-pair populations in a particular molecular eigenstate, and of the extent of consequent overall charge reapportionment within the molecule. The fomer attribute is provided by the extent of atomic excitation into bound hydrogen orbitals contributing to the atomic promotion energy, whereas the latter is provided by the aggregate of these and of contributions from bound Rydberg orbitals and unbound continuum atomic states. This information provides objective quantitative diagnostic descriptions of the effects of chemical interactions on the distributions of states of individual atoms in a molecule, and on the nature of the chemical bonds between them.
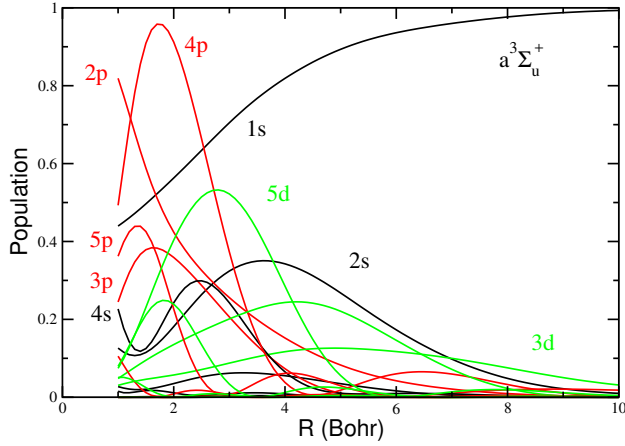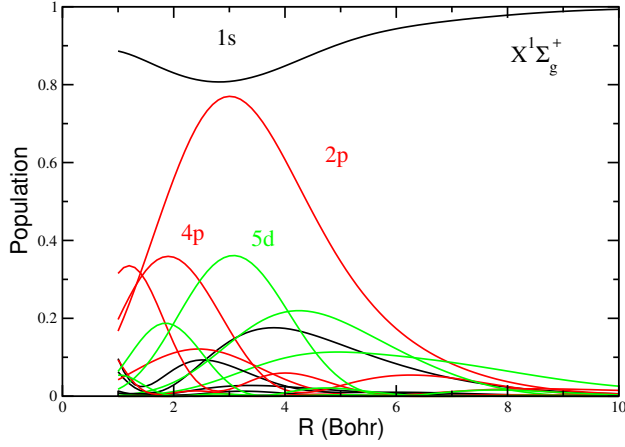
FIG. 10: **Upper Panel**: Atomic hydrogen orbital populations in the ground $X^1\Sigma_g^+$ state of molecular H$_2$. A scale change (X10) has been employed for the excited orbital populations. **Lower Panel**: Atomic hydrogen orbital populations in the $a^3\Sigma_u^+$ excited state of molecular H$_2$. A scale change (X5) has been employed for excited orbital populations except for the 2p state, which is scaled by the factor (X2).

FIG. 11: **Upper Panel**: Atomic hydrogen orbital populations in the $EF^1\Sigma_g^+$ excited state in diatomic molecular hydrogen. **Lower Panel**: Atomic hydrogen orbital populations in the $GK^1\Sigma_g^+$ excited state in diatomic molecular hydrogen. The color codeing employed in identifying the atomic hydrogen eigenorbitals is as in Figure 10.

In Figure 10 are shown atomic hydrogen state populations in the $X^1\Sigma_g^+$ ground state and in the first excited $a^3\Sigma_u^+$ state of molecular hydrogen as functions of atomic separation, calculated employing the one-atom density matrices and the even-tempered atomic-product molecular basis states described in Subsection IV A. The curves for the excited atomic populations in the Upper Panel of Figure 10 are enhanced by the scaling factor (X10) for better visualization, whereas the excited atomic populations in the Lower Panel of Figure 10 are enhanced by the scaling factor (X5), with the exception of the 2p contribution, which is scaled by (X2). A color coding is employed in both Panels of Figure 10 to identify the symmetries of orbital promotions present (s-orbitals are black, p-orbitals are red, d-orbitals are green)

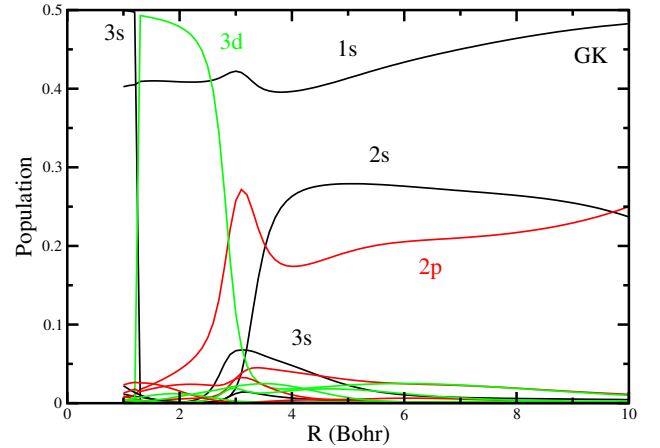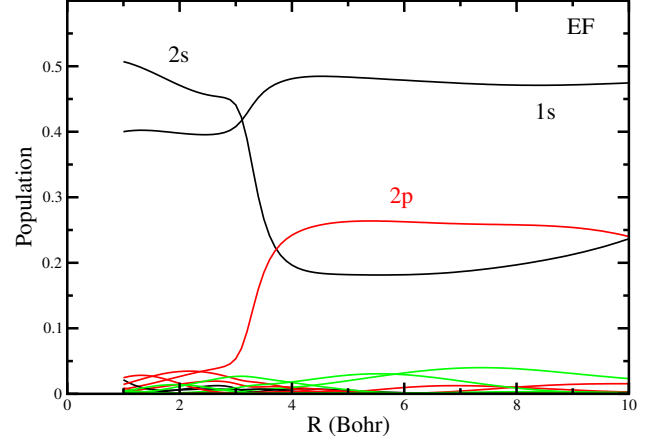There are evident similarities and differences in the

curves reported in the Upper and Lower Panels of Figure 10 for the two molecular states. In the case of the singlet ground state the 1s orbital is seen to be at least 80% occupied at all atomic separations, whereas the 1s population drops to $\approx 45\%$ in the triplet state at smaller interatomic separations, accommodating relatively large 2p promotions in both cases. These behaviors are in accordance with the corresponding atomic promotion energies of Figures 3 and 4. Of course, the variations in atomic populations depicted in Figure 10 ultimately underlie the different behaviors of the atomic promotion energies and interaction energy curves of Figures 3 to 6.

The significant 2p atomic hydrogen orbital populations exhibited in both Panels of Figure 10, second only to that of the dominant 1s orbital, largely determine the nature of bonding in each case. In the singlet state, this 2p contribution becomes smaller at smaller interatomic separa-

tion, whereas in the triplet state the 2p orbital population is still increasing at smaller R values. These behaviors are clearly in accord with the united-atom limits of the singlet and triplet states discussed in the preceeding Subsection IV-A, with the triplet state attaining an energy well above that of the singlet state in this limit [90].

A number of the atomic population curves for bound excited atomic hydrogen p and d states in Figure 10 are seen to exhibit maxima in the general vicinity of the extended bonding region in the $X^1\Sigma_g^+$ state, as well as small recurrences at larger R values, with excited atomic s states apparently contributing in lesser amount. In contrast, the bonding in the triplet state shown in the Lower Panel of Figure 10 is seen to be dominated by a 1s-2p admixture of atomic hydrogen orbitals, with significantly smaller admixtures of other excited hydrogen orbitals.

The individual hydrogen state populations in both Panels of Figure 10 also indicate rather small continuum contributions in molecular hydrogen, reflecting only modest charge transfer contributions to the two lowest-lying molecular states in this homopolar compound [83]. The relatively larger discrete atomic state contributions are quite different for the two molecular states in the 1 to 6 Bohr region, associated with the different bonding characteristics of the states, whereas the population curves exhibit considerable qualitative similarity in the larger R region associated with weak van der Waals attraction [91].

In Figure 11 are shown as examples atomic hydrogen orbital populations in the electronically excited $EF^1\Sigma_g^+$ and $GK^1\Sigma_g^+$ states, which are seen from Figure 7 to both exhibit double well structures. The origins of these features have been discuss qualitatively for some while [104, 105], issues which are here made more quantitative. Specifically, the double well structure in the $EF^1\Sigma_g^+$ total energy curve shown in the Upper Panel of Figure 7 can be attributed to the 2s to 2p population interchange in the 2 to 4 Bohr interval depicted in the Upper Panel of Figure 11, whereas the abrupt decay in the 3d orbital population in the 2 to 3 Bohr interval depicted in the Lower Panel of Figure 11 seemingly accounts for the double well structure in the $GK^1\Sigma_g^+$ total energy curve also shown in the Upper Panel of Figure 11. These quantitative results provide further clarification of the more qualitative earlier discussions of the nature of the double well excited electronic states of diatomic Hydrogen molecules [104, 105].

Finally, it is seen from the Upper Panel of Figure 8 and both Panels of Figure 11 that the $EF^1\Sigma_g^+$ and $GK^1\Sigma_g^+$ states both approach admixtures of 1s (50%), 2s(25%), and 2p(25%) atomic hydrogen orbitals at large values of atomic separation. Accordingly, coherent dissociations of these two states can provide entangled atoms in the original Schrödinger meaning of the word (verschränkung), largely consequent of the exact principle quantum number Coulombic degeneracy in this case. That is, upon dissociation the two hydrogen atoms are regarded as separted non-interacting "subsystems" which are neverthe-
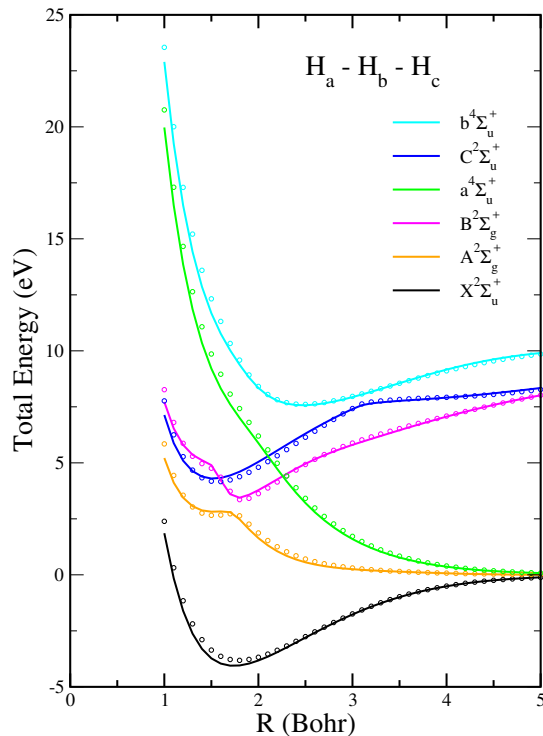

FIG. 12: Electronic energies in symmetric collinear H_3 (H_a-H_b-H_c) (solid lines), in comparison with valence-bond results (circles), calculated employing spectral products of hydrogen spin orbitals on each center, as described in the text.

less still in comunication through the coherent nature of the quantum mechanical description of intially combined subsystems which undergo coherent dissociation. Of course, results reported here in Figures 7 to 11 on basis of atomic spectral representations also provide quantitative descriptions of the atomic "subsystems" of diatomic hydrogen molecules at all geometries examined, not just in coherent dissociation or verschränkung limits. In particular, the preparation of the atomic subsystems is made fully quantitative over the entire course of dissociation on basis of the atomic spectral product methodology reported here.

D. Total electronic, atomic promotion, and interaction energies in triatomic hydrogen molecules

Calculations are reported of total electronic energies, atomic promotion energies, and interaction energies for selected low-lying states of the H_3 molecule in symmetric collinear arrangements (H_a-H_b-H_c). The calculations employ a (1s,2s,3s,2p,3p,3d) basis of fourteen exact hydrogen orbitals on each atom, supplemented with up to
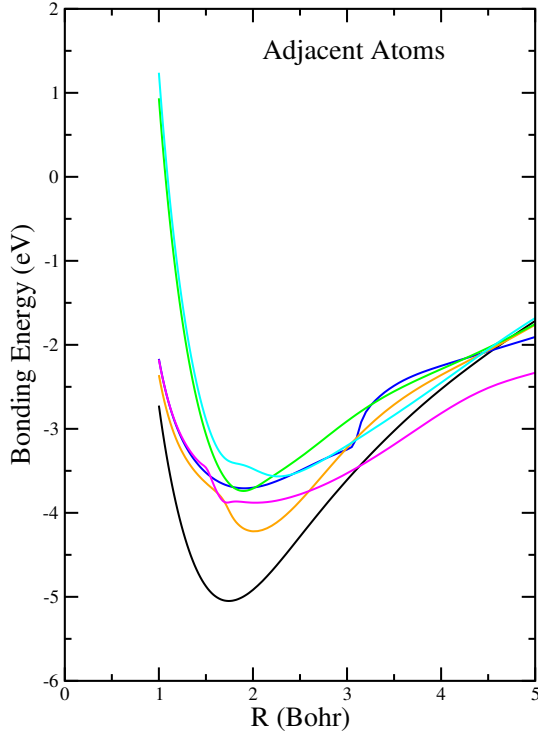
FIG. 13: Interaction energies between adjacent atoms (a-b and b-c) in symmetric collinear H_3 (H_a-H_b-H_c), calculated in the basis sets employed for the total electronic energy calculations shown in Figure 12.

72 of the even-tempered Slater orbitals employed in the H_2 calculations of Figures 1 to 11 to achieve convergence of all quantities for H_3 reported. The particular focus of this illustration is on the complex behaviors of the atomic promotion and interaction energies of the central and two outer atoms as functions of adjacent atom separation ($R=R_{ab}=R_{bc}$) in the H_3 eigenstates considered. These include multiple entanglements among different atoms predicted in the limit of coherent three-body molecular dissociation.

In Figure 12 are shown calculated low-lying total electronic energy curves in comparison with conventional valence-bond values in this basis [89]. The present curves are seen to be in excellent agreement with the valence-bond results, and are also in good accord with other accurate conventional calculations of selected doublet and quartet states [116, 117]. The curves dissociating to three ground-state hydrogen atoms include the $X^2\Sigma_u^+$, $A^2\Sigma_g^+$, and $a^4\Sigma_u^+$ states, whereas the three higher-lying states of $B^2\Sigma_g^+$, $b^4\Sigma_u^+$, and $C^2\Sigma_u^+$ symmetry dissociate to a limit that includes the promotion energy (10.2 eV) of a singly excited hydrogen atom (1s $\rightarrow$ 2s or 2p). These curves are judged to be converged at all R values shown, and

reproduce exactly the correct atomic dissociation limits.

The atomic-pairwise interaction energy curves for adjacent atoms (a-b and b-c) shown in Figure 13 display clearly the consequences of the avoidance between the $A^2\Sigma_g^+$ and $B^2\Sigma_g^+$ states evident in Figure 12, as well as the consequences of a weak avoidance between the $a^4\Sigma_u^+$ and $b^4\Sigma_u^+$ states, which is not particularly apparent in the total energy curves. Specifically, the electronic interaction energy curves between the adjacent atoms in the $A^2\Sigma_g^+$ and $B^2\Sigma_g^+$ states depicted in Figure 13 include abrupt changes as the avoidance region between the two states is traversed in Figure 12 (R = 1.5-2.0 Bohr), with simlar but less pronounced behaviors evident also for the weakly avoiding $a^4\Sigma_u^+$ and $b^4\Sigma_u^+$ states (R= 1.0-1.5 Bohr).

The interaction energy curves for the adjacent atoms in the $X^2\Sigma_u^+$ and $C^2\Sigma_u^+$ states evidently are less structured, although the latter curve shows a noticable deflection and structure in the 3 to 4 Bohr interval, consequent of interaction with a higher lying $^2\Sigma_u^+$ curve not shown [83]. The much weaker interaction energy curves between the two outer atoms (H_a-H_c) in collinear H_3 exhibit related weak structures at smaller R values (not shown).

The Upper and Lower Panels in Figure 14 show the variations of the atomic promotion energies of the outer (a and c) and central (b) atoms, respectively, which complement the interaction-energy curves of Figure 13. Their depiction on a wide range of separations shows both the extent of structures present in the curves over a 25 Bohr interval as well as the asymptotic energy values approached in the limit of three-body molecular dissociation. The many structures shown, particularly for the excited states of Figure 12, are consequent of a sharing of the total promotion energy (10.2 eV) among the three interacting atoms, as well as interactions between states of idential symmetries.

The shapes of the promotion energy curves of all three atoms in the ground $X^2\Sigma_u^+$ state are seen from the two Panels of Figure 14 to be in general accordance with the smooth variation for diatomic H_2 depicted in Figure 3. By contrast, the central and two outer atoms in the avoiding $A^2\Sigma_g^+$ and $B^2\Sigma_g^+$ states in Figure 14 show abrupt energy variations as the avoided crossing region (1.5-2.0 Bohr) in Figure 12 is traversed adiabatically. Also evident over the entire range of separations depicted are compensating complementary variations between the central and outer atomic energies in the three curves, $B^2\Sigma_g^+$, $C^2\Sigma_u^+$, and $b^4\Sigma_u^+$, dissociating to excited atomic states.

The central atom promotion energies of the $B^2\Sigma_g^+$ and $C^2\Sigma_u^+$ states depicted in Figure 14 are seen to approach unphysical $\approx$ 5.0 eV values associated with entangled ground and excited atomic states in the limit of coherent molecular dissociation, whereas the outer atoms in these molecular states approach unphysical $\approx$ 2.7 eV values in Figure 14. These results indicate that repeated ensemble measurements of internal atomic energies in the dissociation limits of these two molecular states will give absolute
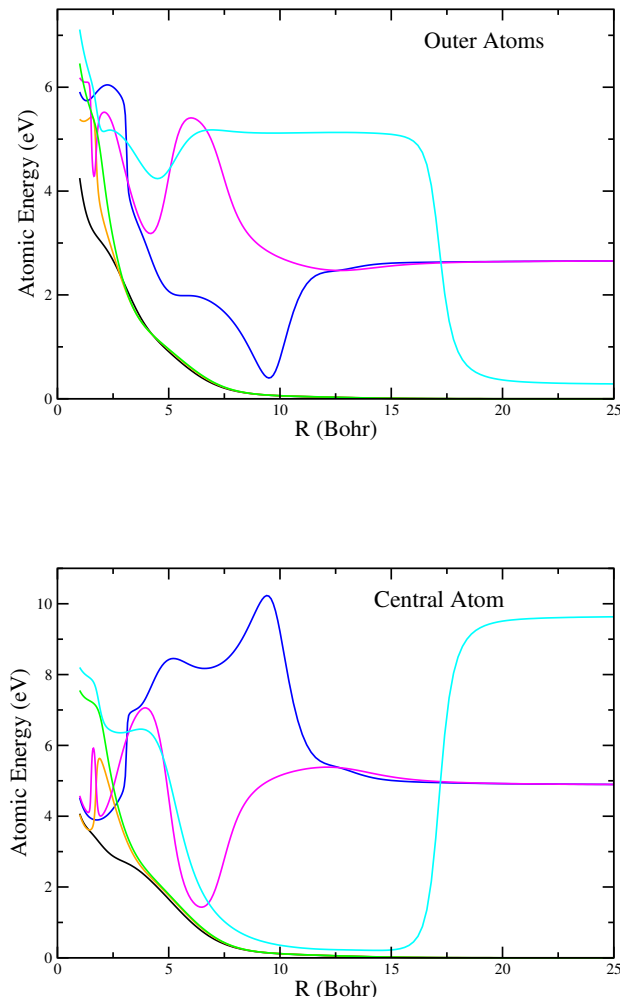
FIG. 14: **Upper Panel**: Atomic promotion energies for the equivalent outer atoms (a and c) in symmetric collinear H_3 calculated in the basis set employed for the total energy curves of Figure 12. **Lower Panel**: Atomic promotion energies for the central atom (b) in symmetric collinear H_3 (H_a-H_b-H_c) calculated in the basis set employed for the total energy curves of Figure 12.

ground (n=1; -13.6 eV) or excited state (n=2; -3.40 eV) hydrogen atom energies with probabilities proportional to the atomic-state populations in the dissociated $B\,^2\Sigma_g^+$ and $C\,^2\Sigma_u^+$ molecular states.

The origins of these interesting large R behaviors are found ultimately in the atomic compositions of the molecular states involved. Specifically, all three atoms in the $B^2\Sigma_g^+$ and the $C^2\Sigma_u^+$ states are found to exhibit mixed populations of ground 1s and excited 2s or 2p atomic hydrogen orbitals in large R limits, a consequence relating to the necessity of having any two of the three atoms remaining in their ground states along these singly excited molecular energy curves. In contrast, the outer and cen-

tral atoms in the $X^2\Sigma_u^+$, $A^2\Sigma_g^+$, $a^4\Sigma_u^+$ molecular curves are seen from Figure 14 to all approach absolute ground (-13.6 eV) state energies, whereas the $b^4\Sigma_u^+$ molecular state approaches an excited (-3.40 eV) atomic energy at large R, in the absence of entanglements in the dissociation processes in these four states.

Although the ground state of triatomic molecular hydrogen is not a chemically stable compound, its three-body photodissociation has been well studied employing stable H_3^+ ions in conjunction with electron pick-up methodolgies [117–121]. Accordingly, the present predictions, reporting atomic-state entanglements having potentially measureable consequences in a simple well-studied triatomic molecule, would seem to provide an opportunity for corresponding experimental studies.

Additional calculation of atomic promotion and interaction energies in low-lying triatomic hydrogen states not reported here, which include three-body dissociation pathways relevant to Dalitz plot geometries conveniently accessible to experimental observations [117–121], have been reported separately elsewhere [91]. These calculations include in particular symmetric C_{3v} triatomic dissociations particularly well-suited for experimental observation in view of the corresponding equilibrium stucture of the precursor H_3^+ ion.

V. DISCUSSION AND CONCLUDING REMARKS

Conventional quantum-chemical calculations of the electronic structures and other attributes of molecules and atomic clusters, performed primarily in the fixed-nuclei Born-Oppenheimer approximation, have evolved to a remarkable degree of sophistication and abundance [22–25], enabled largely but not entirely by continuing improvements in the computational hardware and software available for this purpose. Considerable attention has also been directed at plausible but arguably subjective physical interpretations of the many molecular electronic wave functions, charge density distributions, total electronic energies, and other properties calculated employing such methods [60, 61].

Conceptual advances in these particular connections have seemingly been much less in evidence, with the continuing absence of satisfactory and generally agreed upon *a priori* quantum-mechanical definitions of the properties of atoms in molecules and of the chemical bonds between them, even in the Born-Oppenheimer approximation, resulting in their relegation by knowledgeable theorists to the status of observationally unknowable constructions [3–7]. That is, it has apparently long been assumed that the laws of quantum theory [8, 9], *by themselves*, do not provide unique definitions of such "fragment" molecular properties in the absence of other considerations [6], in spite of early indications to the contrary [122].

In an extension of early work of Eisenschitz and London [70], and of Longuet-Higgen [66], a previously

described universal atomic-eigenstate-based methodology for molecular calculations [70–76, 81–83] has been adopted here to address these fundamental conceptual issues. So-called atomic spectral-product representations of a "van der Waals" subgroup of the molecular symmetric group provide universal Hermitian matrix representatives of the commonly accepted forms of atomic and atomic-interaction operators, and also span totally antisymmetric Schrödinger eigenstates in the absence of *term-by-term* basis antisymmetry.

In this way, a natural partitioning of the total electronic Hamiltonian matrix of a molecule is obtained in terms of *universal* one-atom atomic and two-atom interaction energy matrices. Correspondingly, these atomic and pairwise atomic fragment Hamiltonian matrices, in combination with calculated molecular eigenstates and identification and removal of surious cancelling divergences, provide a total molecular energy expression in the form of sums of well-defined atomic and atomic pairwise bonding contributions, providing an attractive universal *a priori* energy partitioning that follows from the laws of quantum mechanics alone. A conceptual basis is provided therebye for quantitive estimates of atomic "promotion" energies and "net" bonding energies, long made on basis of simple wave function expressions in the absence of more general specific quantum-mechanical prescriptions or definitions of the underlying operators and matrix representatives required for these purposes [10–21].

The wide-spread adoption of many-electron basis sets in term-by-term antisymmetric or essentially equivalent forms commonly employed in the evaluation of molecular Hamiltonian matrices has arguably complicated physical understanding and definitions of atomic operators, their matrix representatives, and their expectation values within molecules. Moreover, such representations apparently do not lead in a simple way to the energy partitioning obtained from an atomic spectral-product representation. It is the case, however, that totally antisymmetric wave functions, no matter how represented, can provide Hermitian fragment atomic and interaction matrices and energies identical with those constructed explicitly in equivalent spectral-product representations [85], emphasizing that the present definitions follow from only the laws of quantum theory and proper representations of self-adjoint atomic operators and their spectral and matrix representatives.

Calculations of the familar electron-pair bonding and anti-bonding states in diatomic hydrogen demonstrate the bounded convergence of the total, atomic, and atomic-interaction electronic energies obtained from the formalism, as well as the seamless partitioning of the total energy into its components in this case. Atomic-state hybridization is accommodated automatically, apportionment of electronic charge among the atoms similarly takes place over the molecular volume via virtual atomic excitations, and the atomic pairwise interaction energy is balanced against the atomic promotion energy in determining the total molecular electronic energy. Ad-

ditionally, charge-transfer effects important in selected excited states of H_2 have been shown previously to be represented by the diffuse neutral atomic state products automatically included in spectral-product representations, in the absence of explict H^-+H^+ charge-transfer configurations [83].

The significant variations of atomic promotion and interaction energies with molecular geometry reported here for the ground and selected excited electronic states of the symmetric collinear H_3 molecule reveal a more nuanced picture of chemical bonding than conventional electronic energy surfaces alone provide. Entangled atomic eigenstates are predicted by the expectation values of individual atomic Hamiltonian operators in the coherent adiabatic dissociation limits of molecular eigenstates. Such results, even in the absence of curve crossings in the simple case of symmetric collinear triatomic hydrogen reported here, are seen to be significantly more complex than the better-known cases of the entangled limits of homo-nuclear diatomic systems [92–103]. Since such three-body dissociations can be achieved experimentally in various ways under appropriate conditions [117–121], an ensemble of measurements of the internal electronic energies of entangled atomic fragments produced by coherent dissociation of polyatomic molecules can potentially report such atomic state distributions for comparisons with theoretical predictions made on basis of the present or other valid computational approaches.

Finally, it should be noted that the atomic spectral product basis employed here, when regarded as a function of both electron and nuclear coordinates, provides a representation suitable for addressing the so-called chemical structure dilemma and its possible resolution [7].

VI. ACKNOWLEDGEMENTS

[1] R.P. Feynman, *Lectures on Physics, 1963*, Vol I, p. 2

[2] K. Ruedenberg and W.H. Eugen Schwartz, "Three millennia of atoms and molecules," in *Pioneers of Quantum Chemistry*, edited by E.T. Strom and A.K. Wilson (ACS Symposium Series: Washington, DC, 2013); Chapter 1, pp. 1-45.

[3] R.G. Parr, P.W. Ayers, and R.F. Nalewajsti, What is an atom in a molecule?, J. Phys. Chem. A **109**, 3957 (2005).

[4] P.-O. Löwdin, "Mathematical definition of a molecule and molecular structure," in *Molecules in Physics, Chemistry, and Biology*, edited by J. Maruani (Reidel, Dordrecht, Holland, 1988), Vol. II, pp. 3-60.

[5] P.-O. Löwdin, On the long way from the Coulombic Hamiltonian to the electronic structure of molecules, Pure and Applied Chemistry, **61**, 2065 (1989).

[6] K. Ruedenberg, The physical nature of the chemical bond, Rev. Mod. Phys. **34**, 326 (1962).

[7] The classical concept of largely fixed geometrical structures of chemically stable molecules provided at the Born-Oppenheimer level of quantum theory has been questioned on basis of significantly different conceptual and computational predictions obtained from proper quantum-mechanical treatment of equivalent nuclei, as described in a continuing series of publications dating from the early work of R.G. Woolley, Quantum theory of molecular structure, Adv. Phys. **25**, 27 (1976), P. Claverie and S. Diner, The concept of molecular structure in quantum theory: Interpretation problems, Int. J. Quantum Chem. **19**, 54 (1979), and E.B. Wilson, On the definition of molecular structure in quantum mechanics, Int. J. Quantum Chem. **S13**, 5 (1979). See also, B.T. Sutcliffe and R.G. Wooley, "On the quantum theory of molecules," in *Fundamental World of Quantum Chemistry: A Tribute to the Memory of Per-Olov Löwdin*, edited by E. Brändas and E.S. Kryachko (Kluwer Academic, Dordrecht, 2004), Vol. 1, pp. 21-63; J. Chem. Phys. **137**, 22A544 (2012); Comment on "On the quantum theory of molecules", J. Chem. Phys. **140**, 037101 (2014), and T. Jecko, On the mathematical treatment of the Born-Oppenheimer approximation, J. Math. Phys. **55**, 053504 (2014), for more recent commentary, and H. Primas, *Chemistry, Quantum Mechanics, and Reductionism: Perspectives in Theoretical Chemistry*, (Springer-Verlag, Berlin, 1983), for additional insights into theories of molecular matter.

[8] P.A.M. Dirac, *The Principles of Quantum Mechanics*, 4th edition (Oxford University Press, London, 1958).

[9] W. Pauli, *General Principles of Quantum Mechanics*, 4th edition (Springer, Berlin, 1980).

[10] L. Pauling, The nature of the chemical bond: Applications of results obtained from the quantum mechanics and from a theory of paramagnetic susceptability to the structures of molecules, J. Am. Chem. Soc. **53**, 1367 (1931).

[11] J.H. Van Vleck, On the theory of the structure of CH_4 and related molecules. Part I, J. Chem. Phys. **1**, 177 (1933).

[12] J.H. Van Vleck, On the theory of the structure of CH_4 and related molecules. Part II, J. Chem. Phys. **1**, 219 (1933).

[13] J.H. Van Vleck, On the theory of the structure of CH_4 and related molecules. Part III, J. Chem. Phys. **2**, 20 (1934).

[14] J.H. Van Vleck, Note on the sp^3 configuration of Carbon, and correction to Part III, J. Chem. Phys. **2**, 297 (1934).

[15] C.A. Coulson, The elctronic structure of methane, Trans. Faraday Soc. (London) **33**, 388 (1937).

[16] C.A. Coulson, Representation of simple molecules by molecular orbitals, Q. Rev. Chem. Soc. **1**, 144 (1947).

[17] P. Ball, Beyond the bond, Nature **469**, 26 (2011).

[18] S.K. Ritter, "Chemical Connections," in *Chemical and Engineering News*, 9 September (2013) Vol. 91, Issue 36, pages 28-33.

[19] R.S. Mulliken, in *Selected Papers of Robert S. Mulliken*, edited by D.A. Ramsay and J. Hinze (University of Chicago Press, Chicago, 1975), p. 451.

[20] C.A. Coulson, *The Spirit of Applied Mathematics* (Clarendon Press, Oxford, 1953), pp. 20-21.

[21] R. Hoffman, "All the ways to have a bond," Eisch Symposium, Bridgehampton University, 29 October 2011 (http://www2.binghamton.edu/chemistry/news/eisch-symposium/hoffman .pdf).

[22] *Theory and Applications of Computational Chemistry*, edited by C.E. Dykstra, G. Frenking, K.S. Kim, and G.E. Scuseria (Elsevier, Amsterdam, 2005).

[23] *Linear-Scaling Techniques in Computational Chemistry and Physics: Methods and Applications*, edited by R. Zaleśny, M.G. Papadopoulis, P.G. Mezey, and J. Leszczynski (Springer, Dordrecht, 2011).

[24] R.G. Parr and W. Yang, *Density Functional Theory of Atoms and Molecules*, (Oxford University Press, New York, 1989).

[25] N.H. March *Electron Density Theory of Atoms and Molecules*, (Academic Press, London, 1992).

[26] C. Edmiston and K. Ruedenberg, Localized atomic and molecular orbitals, Rev. Mod. Phys. **35**, 457 (1963).

[27] W. C. Lu, C. Z. Wang, M. W. Schmidt, L. Bytautas, K. M. Ho, and K. Ruedenberg, Molecule intrinsic minimal basis sets. I. Exact resolution of ab initio optimized molecular orbitals in terms of deformed atomic minimal-basis orbitals. J. Chem. Phy. **120**, 2629 (2004).

[28] A.C. West, M.W. Schmidt, M.S. Gordon, and K. Ruedenberg, A comprehensive analysis of molecular-intrinsic quasi-atomic, bonding, and correlating orbitals. I. Hartree-Fock wavefunctions, J. Chem. Phy. **139**, 234107 (2013).

[29] F. Weinhold and C.R. Landis, *Discovering Chemistry With Natural Bond Orbitals* (John Wiley & Sons, New Jersey, 2012).

[30] F.L. Hirshfeld, Bonded-atom fragments for describing molecular charge densities, Theor. Chem. Acc. **44**, 129 (1977).

[31] P Bultinck, C.V. Alsenoy, P.W. Ayers, R. Carbó-Dorca, Critical analysis and extension of the Hirshfeld atoms in molecules, J. Chem. Phys. **126**, 144111 (2007).

[32] R.F.W. Bader, *Atoms in Molecules; A Quantum Theory* (Oxford University Press, Oxford, 1990).

[33] *The Quantum Theory of Atoms in Molecules*, edited by C.F. Matta and R.J. Boyd (Wiley-VCH Verlag GmbH & Co., Weinheim, 2007)

[34] R.G. Parr, Remarks on the concept of an atom in a molecule and on charge transfer between atoms on molecule formation, Int. J. Quantum Chem. **26**, 687 (1984).

[35] R.F. Nalewajski and R.G. Parr, Information theory, atoms in molecules, and molecular similarity, Proc. Natl. Acad. Sci. USA, **97**, 8879 (2000); J. Rissler, R.M. Novack, and S.R. White, Measuring orbital interaction using quantum information theory, Chem. Phys. **323**, 519 (2006).

[36] J.C. Agulo, J. Antolín, and R.O. Esquivel, "Atomic and Molecular Complexities: Their Physical and Chemical Interpretations", in *Statistical Complexity, Applications in Electronic Structure*, edited by K.D. Sen (Springer, Dordrecht, 2011).

[37] Y. Kurashige, G. Kin-Lic Chan, and T. Yanai, Entangled quantum electronic wavefunctions of the Mn_4CaO_5 cluster in photosystem II, Nature Chemistry, **5**, 660 (2013); K. Boguslawski, P. Tecmer, G. Barcza, Ö. Legeza, and M. Reiher, Orbital entanglement in bond-formation processes, J. Chem. Theory Comput. **9**, 2959 (2013); M. Mottet, P. Tecmer, K. Boguslawski, Ö. Legeza, and M. Reiher, Quantum entanglement in carbon-carbon, carbon-prosphorous, and silicon-silicon bonds, Phys. Chem. Chem. Phys. **16**, 8872 (2014).

[38] J.C. Slater, The virial and molecular structure, J. Chem. Phys. **1**, 687 (1933).

[39] H. Hellmann, *Einfhrung in die Quantenchemie* (Leipzig: Franz Deuticke, 1937) p. 285

[40] R.P. Feynman, Forces in molecules, Phys. Rev. **56** (4), 340 (1939).

[41] J.F. Rico, R López, I Ema, and G. Ramírez, Chemical forces in terms of the electron density, Theor. Chem. Acc. **118**, 704 (2007).

[42] R. McWeeny, Some recent advances in density matrix theory, Rev. Mod. Phys. **32**, 335 (1960).

[43] K. Kitaura and K. Morokuma, A new energy decomposition scheme for molecular interactions in the Hartree-Fock approximation, Int. J. Quantum Chem. **10**, 325 (1976).

[44] T Ziegler and A. Rauk, On the calculation of bonding energies by the Hartree Fock Slater method. I. The transition state method, Theoretica Chimica Acta **46**, 1 (1977).

[45] F. Weinhold, Natural hybrid orbitals, Chem. Phys. **323**, 519 (1980).

[46] R.F.W. Bader, T.T. Nguyen-Dang, and Y. Tai, A topological theory of molecular structure, Rep. Prog. Phys. **44**, 893 (1981).

[47] W. Chen and M.S. Gordon, Energy decomposition analyses for many-body interaction and applications to water complexes, J. Phys. Chem. **100**, 14319 (1996).

[48] A. Gaenko, T.L.Windus, M. Sosonkina, and M.S. Gordon, "Design and Implementation of Scientific Software Components to Enable Multi-scale Modeling: The Effective Fragment Potential (QM/EFP) Method", J. Chem. Comp. Theory, **9**, 222 (2012).

[49] W.E. Palke, The elctronic chemical potential and the H atom in the H_2 molecule, J. Chem. Phys. **72**, 2511 (1980).

[50] M.P. Guse, An atoms in molecules approach to density functional theory, J. Chem. Phys. **75**, 828 (1981).

[51] I. Mayer, A chemical energy component analysis, Chem. Phys. Lett. **332**, 381 (2000).

[52] I. Mayer, Energy partitioning schemes: a dilemma, Faraday Discuss., **135**, 439 (2007).

[53] I. Mayer, On the promotion energy of an atom in a molecule, Chem. Phys. Lett. **498**, 366 (2010).

[54] A.M. Pendas, E. Francisco, and M.A. Blanco, Charge transfer, chemical potentials, and the nature of functional groups: answers from quantum chemical topography, Faraday Discussions, **135**, 423 (2007).

[55] L. Li and R.G. Parr, The atom in a molecule: A density matrix approach, J. Chem. Phy. **84**, 1704 (1986).

[56] J. Rychiewski and R.G. Parr, The atom in a molecule: A wave function approach, J. Chem. Phy. **84**, 1696 (1986).

[57] E. Francisco, A.M. Pendas, and M.A. Blanco, A molecular energy decomposition scheme for atoms in molecules, J. Chem. Theor Comput. **2**, 99 (2006).

[58] A.M. Pendas, M.A. Blanco, and E. Francisco, Chemical fragments in real space: Definitions, properties, and energetic decompositions, J. Comput. Chem. **28**, 161 (2007).

[59] D. Ferro-Costas, A.M. Pendas, L. Gonzalez, and R.A. Mosquera, Beyond the molecular orbital conception of electronically excited states through the quantum theory of atoms in molecules, Phys. Chem. Chem Phys. **16**, 9249 (2014).

[60] *The Chemical Bond: Fundamental Aspects of Chemical Bonding*, edited by G. Frenking and S. Shaik (Wiley-VCH, 2014).

[61] *The Chemical Bond: Bonding Across the Periodic Table*, edited by G. Frenking and S. Shaik (Wiley-VCH, 2014).

[62] B.T. Sutcliffe, What mathematicians know about the solutions of the Schrödinger Coulomb Hamiltonian. Should chemists care? J. Math. Chem. **44**, 988 (2008).

[63] W. Moffitt, Atoms in molecules and crystals, Proc. Roy. Soc. (Lond.) A**210**, 245 (1951).

[64] F.O. Ellison, A method of diatomics in molecules. I. General theory and application to H_2O, J. Am. Chem. Soc. **85**, 3540 (1963).

[65] J.O. Hirschfelder and R.J. Silbey, New type of molecular perturbation treatment, J. Chem. Phys. **45**, 2188 (1966).

[66] H.C. Longuet-Higgins, The symmetry groups of non-rigid molecules, Mol. Phys. **6**, 445 (1963).

[67] J.S. Lomont, *Applications of Finite Groups* (Academic Press, London, 1959).

[68] M. Hammermesh, *Group Theory* (Addison-Wesley, Reading, MA, 1962).

[69] C.D.H. Chisholm, *Group Theoretical Techniques in Quantum Chemistry* (Academic Press, London, 1976).

[70] H. Eisenschitz and F. London, On the ratio of the van der Waals forces and the homo-polar binding forces, Z. Physik **60**, 491 (1930).

[71] P.W. Langhoff, Spectral theory of physical and chemical binding, J. Phys. Chem. **100**, 2974 (1996).

[72] P.W. Langhoff, R.J. Hinde, J.A. Boatz, and J.A. Sheehy, Spectral theory of the chemical bond, Chem. Phys. Lett. **358**, 231 (2002).

[73] P.W. Langhoff, J.A. Boatz, R.J. Hinde, and J.A. Sheehy, Atomic spectral methods for molecular electronic structure calculations, J. Chem. Phys. **121**, 9323 (2004). The energy partitioning of Eqs. (50) to (52) in this reference are based on the definitions of atomic and pairwise-atomic interaction Hamiltonian matrices in terms of spectral-product expressions provided in Eq.

(34) and the equivalence demonstrated in Eqs. (66) to (69) therein, as described in further detail in the present report.

[74] P.W. Langhoff, R.J. Hinde, J.D. Mills, and J.A. Boatz, Spectral-product methods for electronic structure calculations, Theor. Chem. Acc. **120**, 194 (2008).

[75] M. Ben-Nun, J.D. Mills, R.J. Hinde, C.L. Winstead, J.A. Boatz, G.A. Gallup, and P.W. Langhoff, Atomic spectral-product representations of molecular electronic structure: Metric matrics and atomic-product compositions of molecular eigenfunctions, J. Phys. Chem. **113**, 7687 (2009).

[76] P.W. Langhoff, J.D. Mills, and J.A. Boatz, Atomic-pair theorem for universal matrix representatives of molecules and atomic clusters in non-relativistic Born-Oppenheimer approximation, J. Math. Phys. (submitted for publication).

[77] The atomic eigenfunctions in the outer product of Eq. (1) are described in a set of commonly-oriented coordinate systems centered at the atomic nuclei, the axes of which remain parallel to the laboratory frame independent of the magnitude and direction of the atomic separation vectors $\boldsymbol{R}_{\alpha\beta} \equiv \boldsymbol{R}_{\beta} - \boldsymbol{R}_{\alpha}$. The orthonormality of the entire product basis is consequent of the disjoint configuration space coordinates of the electrons assigned to individual nuclei and measured therefrom, in spite of which the individual atomic electrons can access the entire physical spatial region of a molecule.

[78] R. McWeeny, *Methods of Molecular Quantum Mechanics*, 2nd Edition (Academic, London, 1989).

[79] The appearance of non-zero diagonal and off-diagonal dissociation limits of Eqs. (12) and (13) are consequent of atomic-state symmetries alone; E. Wigner and E.E. Witmer, On the structure of the spectra of two-atom molecules according to quantum mechanics, Z. Physik **51**, 859 (1928).

[80] Each of the solutions of the many-electron (Coulombic) atomic or molecular Schrödinger equation are at least 2^{n_e}-fold degenerate, where n_e is the number of electrons. This Lemma follows, for example, from factoring into a product of spin and spatial terms the most general form of a complete spin-orbital product representation of many-electron states [66]. Most of these degenerate solutions are so-called non-Pauli states, which can be made to transform under irreps of the n_e-electron symmetric group *other* than the totally antisymmetric irreducible representation [66–68]. The origins and natures of these states have been described in some detail [72–74], and from another perspective by J.D. Morgan and B. Simon, Behavior of molecular potential energy curves for large nuclear separations, Int. J. Quantum Chem **17**, 1143 (1980); W.H. Adams, Perturbation theory of intermolecular interactions: What is the problem, are there solutions? ibid. **38, S24**, 531 (1990). See also, J.D. Mills and P.W. Langhoff, *"On the Non-Pauli States of Atoms and Molecules,"* Annual Meeting of the California-Nevada Section of the American Physical Society, Cal Poly, San Luis Obispo, CA, 2-3 November 2012.

[81] P.W. Langhoff, J.A. Boatz, R.J. Hinde, and J.A. Sheehy, "Spectral theory of chemical bonding", in *Low-Lying Potential Energy Surfaces*, edited by M.R. Hoffmann and K.G. Dyall (ACS Symposium Series 828, Washington, DC, 2002), Chapter 10, pp. 221-237.

[82] P.W. Langhoff, J.A. Boatz, R.J. Hinde, and J.A. Sheehy, "Applications of Löwdin's metric matrix: Atomic spectral methods for electronic structure calculations," in *Fundamental World of Quantum Chemistry: A Tribute to the Memory of Per-Olov Löwdin*, edited by E. Brändas and E.S. Kryachko (Kluwer Academic, Dordrecht, 2004), Vol. 3, pp. 97-114. Comments similar to those made in reference [73] herein also apply to Eqs. (10) to (22) of this reference.

[83] J.D. Mills, M. Ben-Nun, K. Rollin, M.W.J. Bromley, Jiabo Li, R.J. Hinde, C.L. Winstead, J.A. Sheehy, J.A. Boatz, and P.W. Langhoff, Atomic Spectral Methods for Ab-Initio Molecular Electronic Energy Surfaces: Transitioning From Small-Molecule to Biomolecular-Suitable Approaches, J. Phys. Chem. B **120**, 8321 (2016); P.W. Langhoff, "Atomic Spectral-Product Methods for Molecular Electronic Structure Calculations: Bridging the Gap to Large Atomic Aggregates," *49th Symposium on Theoretical Chemistry, University of Erlangen, Erlangen, DE,* 22-26 September 2013; P.W. Langhoff, *Computational Implementation of Spectral Theroy*, SBIR Final Report, US Air Force Research Laboratory, AFRL-RZ-ED-TR-113, 1687-7697 (2009).

[84] P.-O. Löwdin, On the nonorthogonality problem connected with the use of atomic wave functions in the theory of molecules and crystals, J. Chem. Phys. **18**, 365 (1950); On the nonorthogonality problem, Advan. Quantum Chem. **5**, 185-198 (1970); A. Szabo and N.S. Ostland, *Modern Quantum Chemistry: Introduction to Advanced Structure Theory* (Macmillan, London, 1982) pp. 142-145.

[85] Methods for transforming between diatomic molecular eigenfunctions represented in the spectral-product basis of Eq. (1) and those obtained from more conventional antisymmetrized orbital-product or other representations have been discussed previously[73, 74]. See also in this connection, J.M. Spotts, C.-K. Wong, M.S. Johnson, M. Okumura, J.A. Boatz, R.J. Hinde, J.A. Sheehy, and P.W. Langhoff, Multi-photon ionization spectroscopy of $AlAr_N$ clusters, J. Phys. Chem. A **107**, 6948 (2003), for alternative construction of spectral-product representations from diatomic wave functions obtained employing conventional quantum-mechanical calculations. Although similar transformation procedures can be employed for polyatomic molecules, much of the computational advantage of the spectral-product development is lost in such a "projection" approach [72].

[86] The divergence of continuum contributions to the atomic energies of Eq. (19), as well as to the interaction energies of Eq. (20), are consequent of the relatively weak decay of the amplitudes of Couloub waves with increasingly large atomic energy, which decay is insufficiently rapid to overcome the linear increase included in the spectral integral expectation values; see, for example, Hans A. Bethe and Edwin Salpeter, *Quantum Mechanics of One- and Two-Electron Atoms* (Springer-Verlag, Berlin, 1957), pp. 21-47. The divergent atomic terms in Eq. (19) are easily identified, whereas those of the interaction energy of Eq. (20) include cross terms involving bound and contiuum atomic states which require careful numerical evaluation and analytical treatment. The equivalence of the cancelling atomic and atomic interaction terms is accomplished analytically by re-expressing the latter terms employing Virial Theo-

rem [38] considerations. Such divergent terms are arguably resonsible for the large range of estimated values of fragment energies obtained employing many of the previouly reported disparate formalism devised for this purpose [47–61]. These estimates generally employ finite-basis L^2 molecular wave functions which implicitly include atomic continuum terms, providing finite but possibly surious values.

[87] K. Ruedenberg, R. C. Raffenetti, R. D. Bardo, "Energy, Structure, and Reactivity," in *Proceedings of the 1972 Boulder Summer Research Conference on Theoretical Chemistry*, (Ed. D. W. Smith, Wiley, N. Y., 1973) p. 164.

[88] D.P. Chong, E.V. Lanthe, S. van Gisbergen, and E.J. Baerrends, Even-tempered Slater-type orbitals revisited: From hydrogen to krypton, J. Comp. Chem. **25**, 1030 (2004).

[89] G.A. Gallup, *Valence Bond Methods, Theory and Applications* (Cambridge University Press, Cambridge, 2002) (http://molcrunch.sourceforge.net/)

[90] *NIST Atomic Spectral Data Base* (physicsnist.gov/PhysRefData/index.html).

[91] P.W. Langhoff, J.D. Mills, J.A. Boatz, and G.A. Gallup, "Quantum-Mechanical Definition of Atoms and Bonds in Molecules," *50th Symposium on Theoretical Chemistry, University of Vienna, Vienna, DE,* 14-18 September 2014.

[92] M. Schlosshauser, *Decoherence and the Quantum-to-Classical Transformation* (Springer-Verlag, Berlin, 2007).

[93] A. Gonis, X.-G. Zhang, D.M. Nicholson, and G.M. Stocks, Energy convexity as a consequence of decoherence and pair-extensive interactions in many-electron systems, J. Phys. Chem. Solids **75**, 680 (2014); Self-entanglement and the dissociation of homonuclear diatomic molecules, Mol. Phys. **112**, 453 (2014).

[94] E.S. Fry and T. Walther, "Fundamental Tests of Quantum Mechanics" in, *Advances in Atomic, Molecular and Optical Physics* **42**, 1 (2000).

[95] X.X. Yi and W. Wang, Creating entangled atomic pairs by photodissociation, J. Phys. B **34**, 5087 (2001).

[96] B. Zhao, Z.-B. Chen, J.-W. Pan, L. Schmiedmayer, A. Recati, G.E. Astrakharchik, and T. Calarco, High-fidelity entanglement via molecular dissociation in integrated atom optics, Phys. Rev. A **75**, 042312 (2007).

[97] C. Gneiting and K. Hornberger, Molecular Feshbach dissociation as a source for motionally entangled atoms, Phys. Rev. A **81**, 013423 (2010).

[98] T. Odagiri, T. Tanabe, and N. Kouchi, Dynamics of entangled H(2p) pair generated in the photodissociation of H_2, J. Phys. Conference Series **388**, 012024 (2012).

[99] V. Letokhov, *Laser Photoionization Spectroscopy* (Elsevier, Atlanta, GA, 2012).

[100] S. Arai, T. Kamosaki, M. Ukai, K. Shinsaka, Y. Hatano, Y. Ito, H. Koizumi, A. Yagishita, K. Ito, K. Tanaka, Lyman α, Lyman α coincidence detection in the photodissociation of doubly excited molecular hydrogen into two H(2p) atoms, J. Chem. Phys. **88**, 3016 (1988).

[101] T. Tanabe, T. Odagiri, M. Nakano, Y. Kumagai, I.H. Suzuki. M. Kitajima, and N. Kouchi, "Effect of entanglement on the decay dynamics of a pair of H(2p) atoms due to spontaneous emission," Phys. Rev. A **82**, 04010 (2010).

[102] P. Sancho and L. Plaja, Comment on "Effect of entan-

[103] T. Tanabe, T. Odagiri, M. Nakano, Y. Kumagai, I.H. Suzuki. M. Kitajima, and N. Kouchi, Reply to Comment on "Effect of entanglement on the decay dynamics of a pair of H(2p) atoms due to spontaneous emission," Phys. Rev. A **83**, 066102 (2011).

[104] W. Moffitt, Atomic Valence States and Chemical Binding, Rept. Prog. Phys. **17**, 173 (1954).

[105] R. S. Mulliken, The Rydberg states of molecules: VI. Potential energy curves and dissociation behavior of (Rydberg and other) diatomic states, J. Chem. Phys. **45**. 509-514 (1966).

[106] L. Wolniewicz and K. Dressler, "Adiabatic potential curves and nonadiabatic coupling functions for the first five excited $^1\Sigma_g^+$ states of the hydrogen molecule," J. Chem. Phys. **100**, 444-451 (1994).

[107] G. Staszewska and L. Wolniewicz, "Adiabatic energies of excited $^1\Sigma_u^+$ states of the hydrogen molecule" J. Mol. Spectroscopy **212**, 208-212 (2001).

[108] U. Frantz, D. Wünderlich, Franck-Condon Factors, Transition Probabilities, and Radiative Lifetimes for Hydrogen molecules and their Isotopomers, At. Data Nucl. Data Tables, **92**, 853-973 (2006).

[109] J.D. Mills, J.A. Boatz, and P.W. Langhoff, "Atomic entanglements in three-body molecular dissociation," APS National Meeting, Los Angles, CA 5-9 March (2018).

[110] P.W. Langhoff, "Atomic Spectral-Product Methods for Molecular Electronic Structure Calculations: Bridging the Gap to Large Atomic Aggregates," *49th Symposium on Theoretical Chemistry, University of Erlangen, Erlangen, DE,* 22-26 September 2013.

[111] I.D. Petsalakis, G. Theodorakopoulos, and J.S. Wright, Theoretical calculations on electronic transitions for H_3, including Rydberg and transition state spectra, J. Chem. Phys. **89**, 6850 (1988).

[112] T. Tanabe, T. Odagiri, M. Nakano, Y. Kumagai, I.H. Suzuki. M. Kitajima, and N. Kouchi, "Effect of entanglement on the decay dynamics of a pair of H(2p) atoms due to spontaneous emission," Phys. Rev. A **82**, 04010 (2010).

[113] P. Sancho and L. Plaja, Comment on "Effect of entanglement on the decay dynamics of a pair of H(2p) atoms due to spontaneous emission," Phys. Rev. A **83**, 066101 (2011).

[114] T. Tanabe, T. Odagiri, M. Nakano, Y. Kumagai, I.H. Suzuki. M. Kitajima, and N. Kouchi, Reply to Comment on "Effect of entanglement on the decay dynamics of a pair of H(2p) atoms due to spontaneous emission," Phys. Rev. A **83**, 066102 (2011).

[115] T. Odagiri, T. Tanabe, and N. Kouchi, Dynamics of entangled H(2p) pair generated in the photodissociation of H_2, J. Phys. Conference Series **388**, 012024 (2012).

[116] Z. Peng, S. Kristyan, and A. Kuppermann, Excited electronic potential-energy surfaces and transition moments for the H_3 system, Phys. Rev. A **52**, 1005 (1995).

[117] U. Galster, F. Baumgartner, U. Müller, H. Helm, and M. Jungen, Experimental and quantum-chemical studies on the three-particle fragmentation of neutral triatomic hydrogen, Phys. Rev. A **72**, 062506 (2005).

[118] P.C. Cosby and H. Helm, Photodissociation of triatomic hydrogen, Phys. Rev. Letts. **61**, 298 (1988).

[119] U. Galster, P. Kaminski, M. Beckert, H. Helm, and

U. Müller, Kinematically complete final state investigations of molecular photodissociation: two- and three-body decay of laser-prepared H_3 3s $^2A'_a$, Eur. Phys. J. D **17**, 307 (2001).

[120] U. Galster, U. Müller, M. Jungen, and H. Helm, Nonadiabatic coupling and vector correlation in dissociation of triatomic hydrogen, Faraday Discuss. **127**, 439 (2004).

[121] C.M. Laperle, J.E. Mann, T.G. Clements, and R.E. Continetti, Experimentally probing the three-body predissociation dynamics of the low-lying Rydberg states of H_3 and D_3, J. Phys. Conference Series **4**, 111 (2005).

[122] H.I. Metiu, Localization of electrons in molecules, Phys. Rev. A **2**, 13 (1970).